

Analysis Note for the STAR Publication: *“Beam Energy Dependence of the Third Harmonic of Azimuthal Correlations in Au+Au Collisions at RHIC”*

PA's: Paul Sorensen, Niseem Magdy, Yadav Pandit, Navneet Kumar Pruthi, Hui Wang and Liao Song.

<https://drupal.star.bnl.gov/STAR/content/bes-v3-paper-proposal>

This Analysis note covers the following topics:

Data sets and QA

Event and track selection criteria

Analysis procedure

 Observable

 Corrections and efficiency

 Removing short range correlations

Systematic uncertainty estimates

 Variations with time and analysis cuts

 Comparisons to other methods

Figures

Auxiliary studies

 dN/d η parameterizations

 pions only

 ET-ET correlations

 Model comparisons

Data sets and QA:

We've analyzed data from 7.7, 11.5, 14.5, 19.6, 27, 39, 62.4, and 200 GeV. For the 200 GeV data analysis we've used Run 4 data and Run 11 data. For the 62.4 GeV analysis, we've attempted to use run 10 data but found the data set to be of such poor quality that we rely only on Run 4 data for 62.4 GeV. The primary problem for this data set seems to be related to the sector that was masked out. Although this is a safe step for preventing bad results for high pt spectra, it's disastrous for correlations analyses.

The remaining energies were taken in the 2010, 2011, and 2014 BES-I runs.

This analysis makes use of the binary data sets generated by Hui Wang. As such, the QA and data set information is identical to that in the STAR notes: https://drupal.star.bnl.gov/STAR/system/files/balance_analysis_notes_v1.07.pdf

The list of good runs can be found at:

<http://www.star.bnl.gov/protected/bulkcorr/wanghui6/Run list/7GeV.txt>

<http://www.star.bnl.gov/protected/bulkcorr/wanghui6/Run list/11GeV.txt>

<http://www.star.bnl.gov/protected/bulkcorr/wanghui6/Run list/14GeV.txt>

<http://www.star.bnl.gov/protected/bulkcorr/wanghui6/Run list/19GeV.txt>

<http://www.star.bnl.gov/protected/bulkcorr/wanghui6/Run list/27GeV.txt>

<http://www.star.bnl.gov/protected/bulkcorr/wanghui6/Run list/39GeV.txt>

<http://www.star.bnl.gov/protected/bulkcorr/wanghui6/Run list/62GeV.txt>

<http://www.star.bnl.gov/protected/bulkcorr/wanghui6/Run list/200GeV run11.txt>

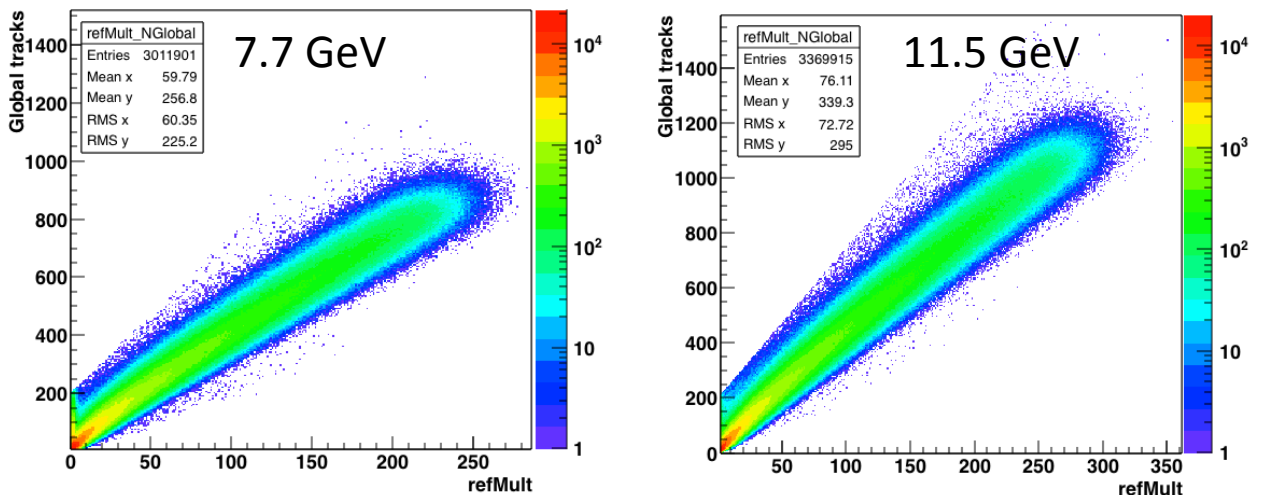
Below, we tabulate the total number of events analyzed for each energy after cuts and QA. In some cases, the best portions of data sets have been analyzed. Especially where statistical errors were not problematic, we've focused on data quality over quantity.

200 GeV	62.4	39	27	19.6	14.5	11.5	7.7
300M	4M	10M	19M	16M	18M	3.5M	3M

Event and Track selection criteria:

The z-vertex ranges allowed in the analysis varies with energy. The choices were made to balance the need for statistics vs reducing systematic biases arising from variation with z-vertex. We apply a $|Vz| < 2$ cm cut (1cm for 14.5 GeV) and an energy dependent NtracksGlobal vs refMult cut. For all but the 2004 data, we require at least two tracks to have a TOF matched hit. Track cuts are varied to estimate the systematic uncertainties but the standard cuts include $p_T > 0.2$ GeV, $|\eta| < 1$, $N_{\text{hits}} > 15$ and $DCA < 3.0$ cm.

7.7 GeV	$ Vz < 40$ cm	$N_{\text{Global}} < (200 + 5.5 * \text{refMult})$
11.5	40	$N_{\text{Global}} < (200 + 5.5 * \text{refMult})$
14.5	40	$N_{\text{Global}} < (200 + 5.5 * \text{refMult})$
19.6	40	$N_{\text{Global}} < (200 + 5.5 * \text{refMult})$
27	20	$N_{\text{Global}} < (200 + 5.5 * \text{refMult})$
39	40	$N_{\text{Global}} < (200 + 5.5 * \text{refMult})$
62.4	20	-----
200	20	TOFmatchedTrack > 2



Analysis Procedure:

We calculate the two-particle cumulant $v_3^2\{2\}$ which is the third Fourier harmonic of the two particle correlations.

$$v_n^2\{2\} = \langle \cos n(\varphi_1 - \varphi_2) \rangle - \langle \cos n\varphi_1 \rangle \langle \cos n\varphi_2 \rangle - \langle \sin n\varphi_1 \rangle \langle \sin n\varphi_2 \rangle$$

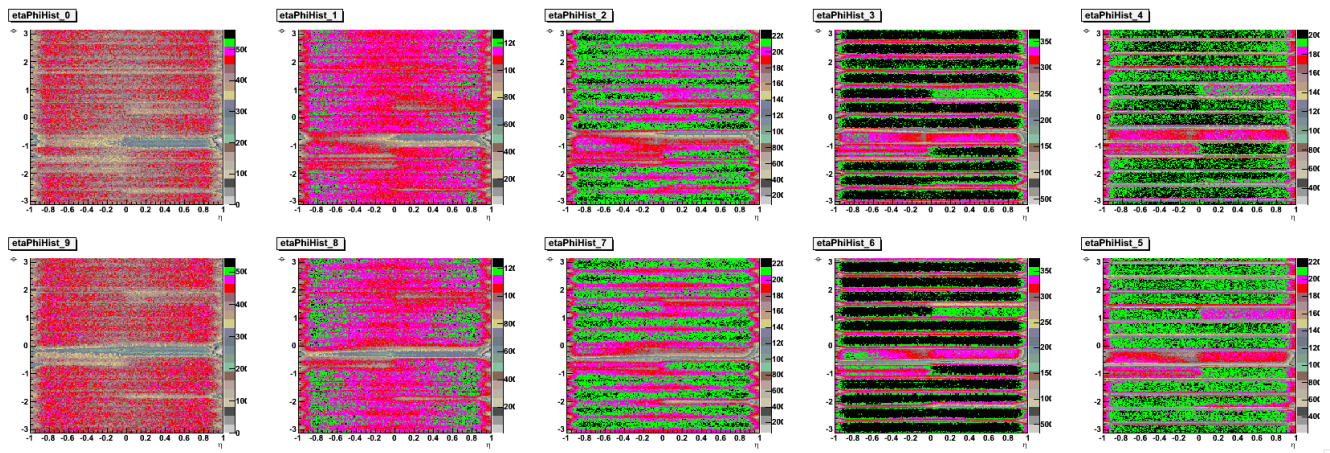
$$\langle \cos n(\varphi_1 - \varphi_2) \rangle = \frac{1}{N_{ev}} \sum_{N_{ev}} \left(\frac{\sum_{i=0}^N \sum_{j=i+1}^N w_i w_j \cos n(\varphi_i - \varphi_j)}{\sum_{i=0}^N \sum_{j=i+1}^N w_i w_j} \right)$$

Our results are binned vs $\Delta\eta$. w_i and w_j are track-by-track weights that are used to correct for detector acceptance and efficiency. We apply track-by-track weights because the usual single particle corrections $\langle \cos 3\varphi \rangle$ averaged over all acceptance do not work when looking at the correlation functions differentially. To overcome this, we've developed the weighting procedure which has the benefit of being able to correct for efficiency as well. The weighting procedure involves first binning particles in φ and η and averaging over all events. Since acceptance will depend on particle charge, track curvature (related to p_T), z-vertex, and centrality, we create separate η vs φ histograms for events with different z-vertex, centrality, and magnetic field when appropriate, and for tracks with different sagita (curvature) and charge. z-vertex bins are 20 cm wide with selections from $-40 < Vz < -20$, $-20 < Vz < 0$, $0 < Vz < 20$, $20 < Vz < 40$. Narrower bins were tried where statistics were available but did not change the results. We use the standard centrality definitions to divide up our weights by centrality. The Sagita of a track is calculated from it's p_T , the size of the TPC and the magnetic field. The sagita is: $S = \text{charge} * ((20.*p_T/3.) - \sqrt{(\text{pow}(20.*p_T/3., 2.) - \text{pow}(0.75, 2.))})$. See note at the end of the document for more details. The sagita is then binned according to $S < -20, -15, -10, -5, 0, 5, 10, 15, 20$ or $S > 20$ which defines 10 bins that cover 5 different p_T ranges for 2 different charges.

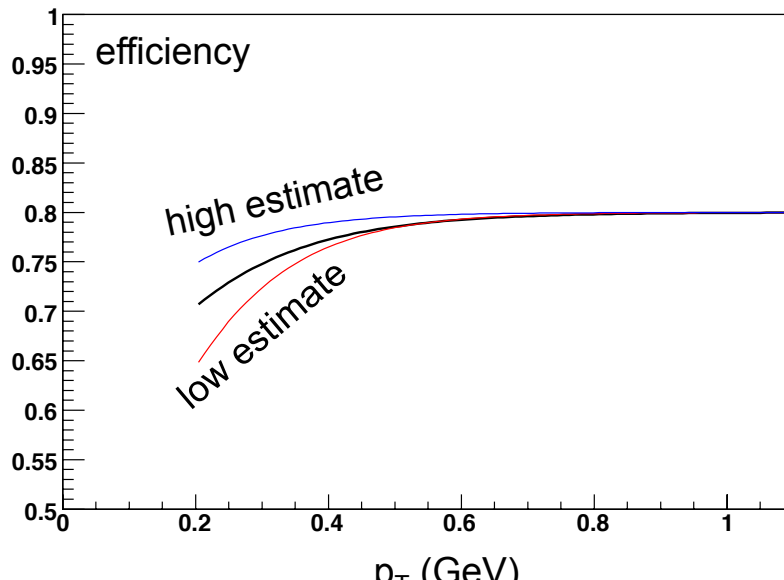
Once those histograms are filled and averaged over all events, the histograms are normalized. Then the weight w_i for a given track is taken as $1/(\text{eff} * \text{binCont})$ where binCont is the content of the bin corresponding to that track and eff is the p_T dependent efficiency determined from embedding. We vary the efficiency estimate to test the dependence on efficiency and to estimate systematic errors.

Analysis Procedure:

Below we show an example of the η, ϕ weights for one centrality and one energy. The top row shows negatively charged track distributions, the bottom row shows positively charged track distributions. The left side has the largest sagita (curvature) and therefore the lowest p_T , the right bins have the smallest curvature (highest p_T). The less curved tracks clearly show the effect of sector boundaries while the more curved tracks are less likely to be lost in sector boundaries. The histograms clearly illustrate that the acceptance depends strongly on η and ϕ .

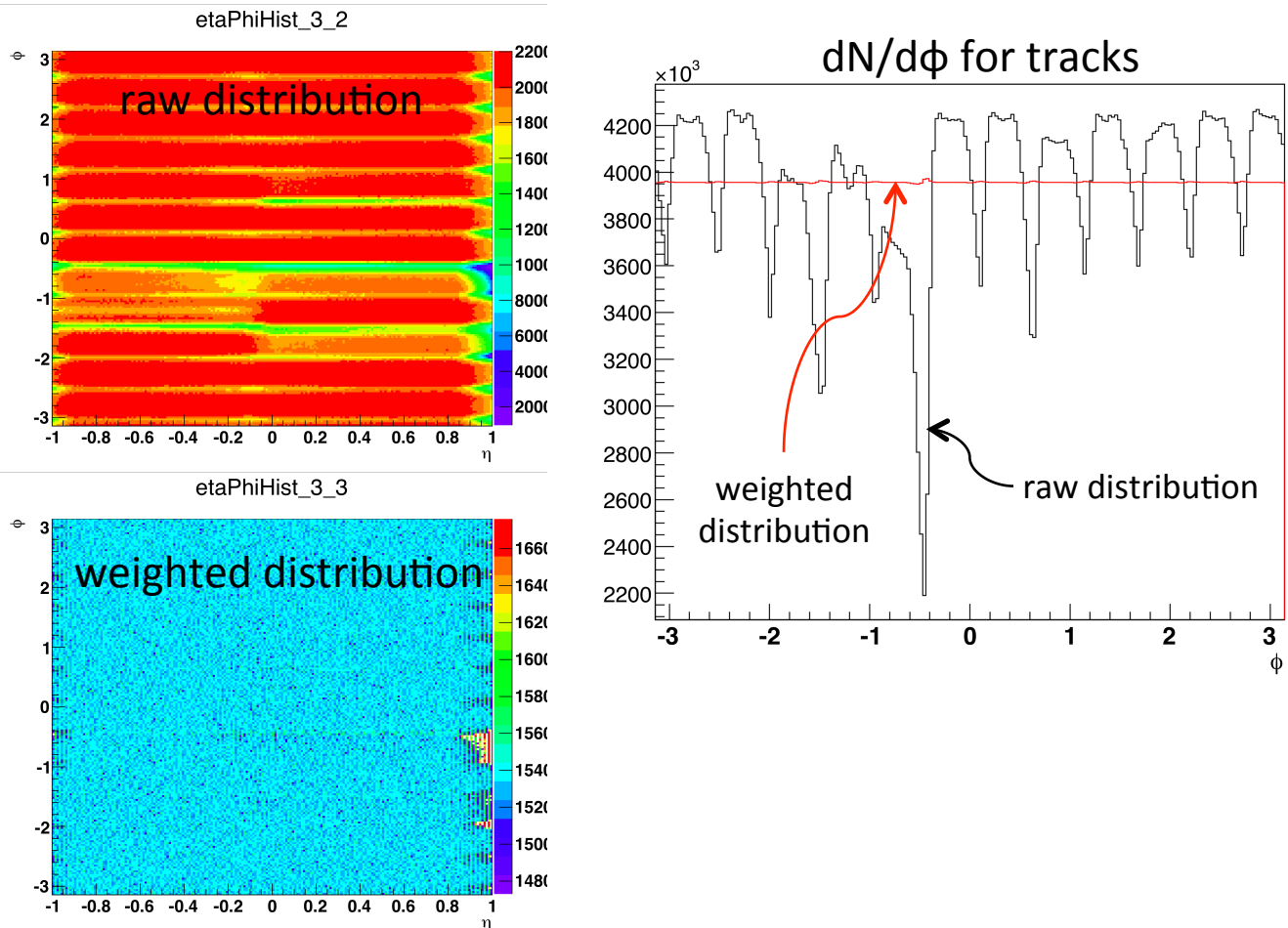


Below, we also show the efficiency parameterizations we use to correct for the p_T dependent efficiency. The black curve is a fit to efficiency from embedding. The blue and red show two extremes that were used to estimate systematic uncertainties. Only the p_T dependence of the efficiency matters since a constant efficiency offset will cancel out in the numerator and denominator for this analysis.



Analysis Procedure:

After weighting, we verify that the distribution of tracks is flat. Once the $v_n\{2\}$ data has been corrected for acceptance with weights, the residual corrections $\langle \cos n\phi \rangle^2 + \langle \sin n\phi \rangle^2$ are also verified to be very small (in almost all cases consistent with zero and in all cases smaller than a few % of the signal).

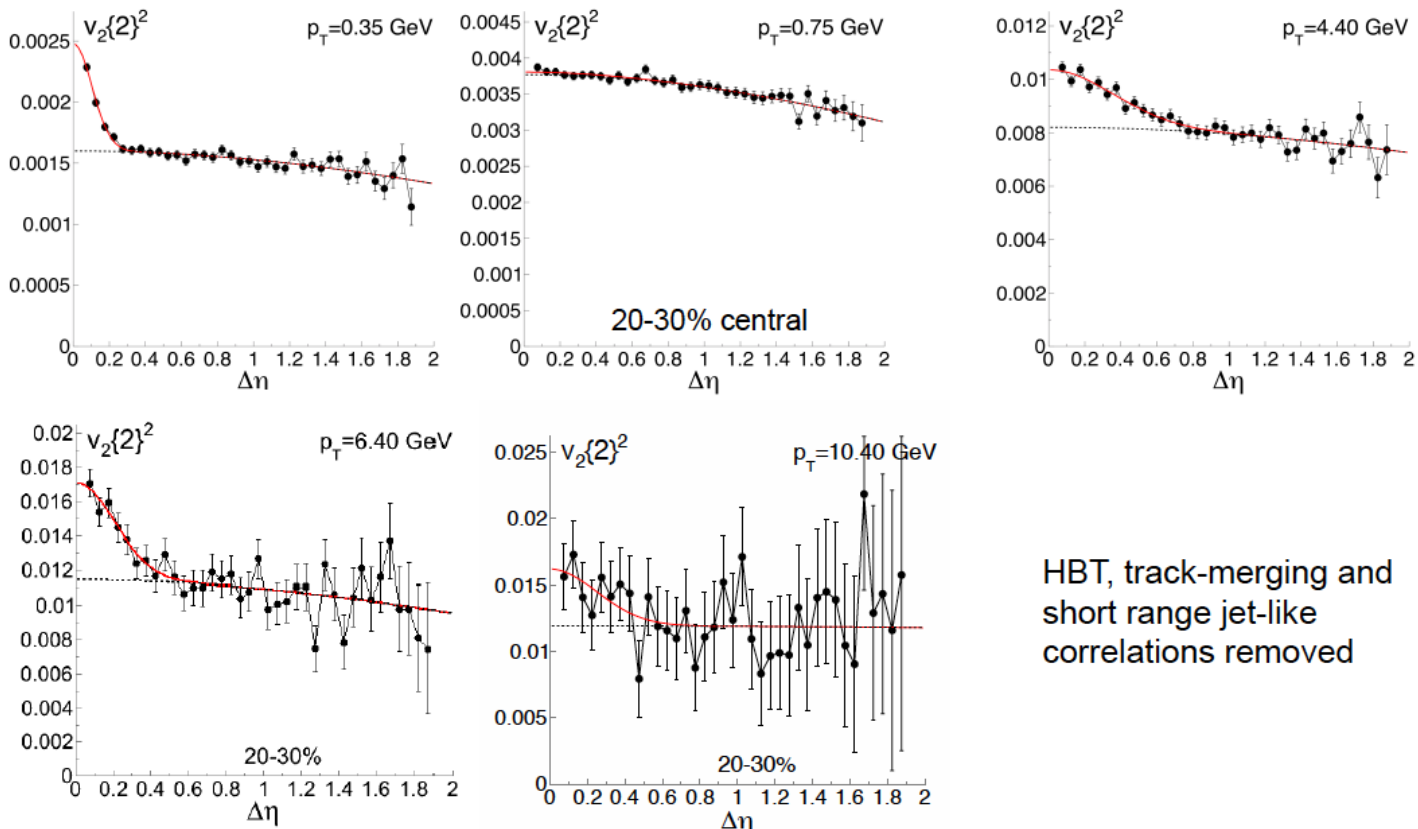


Not all holes in the acceptance can be corrected. Especially just on the edge of the acceptance. These holes affect a very small fraction of the pairs of tracks though so their affect is negligible as can be assessed from the $\langle \cos n\phi \rangle^2 + \langle \sin n\phi \rangle^2$ correction.

Analysis Procedure:

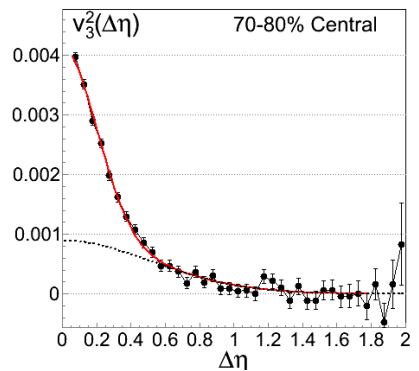
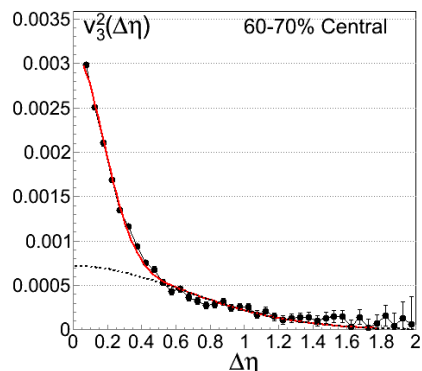
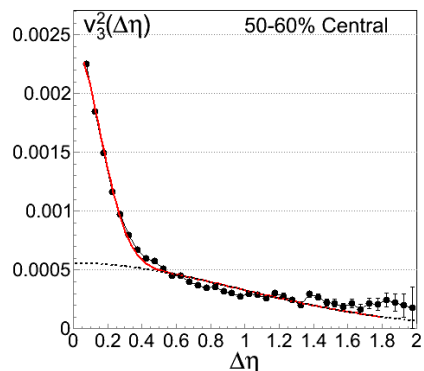
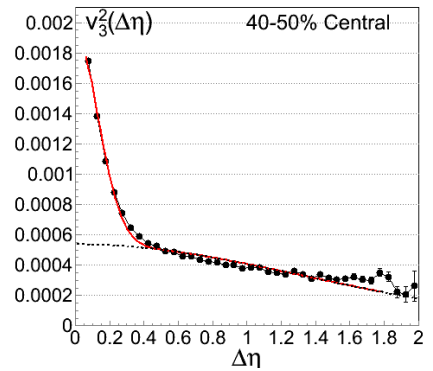
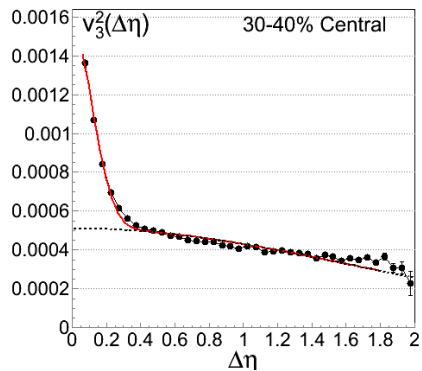
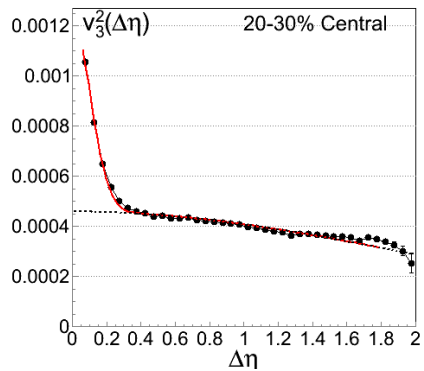
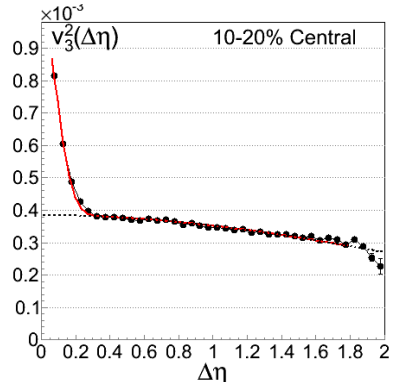
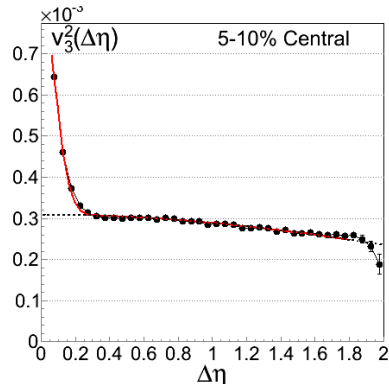
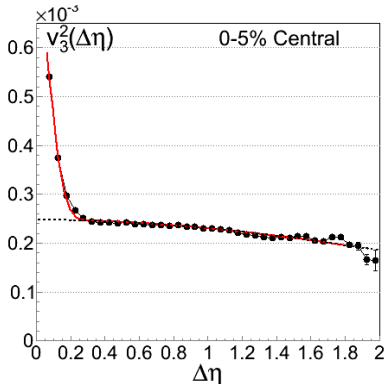
Once the $v_n\{2\}$ data has been corrected for acceptance with weights, we can plot $v_n\{2\}$ vs $\Delta\eta$ to investigate the behavior of the correlation functions. The first bin shows a strong anti-correlation due to track merging. For this reason, we neglect that bin. A narrow peak centered at zero is observed which is due to HBT like correlations. It goes away as the momentum is slightly increased. It can also be made to disappear depending on the charge or particle type used (identical particles have the strongest quantum interference pattern). Once p_T is increased, at high enough p_T , a jet like peak does begin to appear (see below). For part of our analysis we calculate the average $v_n\{2\}$ averaged over $\Delta\eta$ and use the fit function to subtract off the narrow HBT peak and the contribution from track merging. Then the long-range structure is reported as $\langle v_n\{2\} \rangle$. We assign an error on the subtraction of the narrow peak of 10%. The complete set of fits is shown on the following pages. For peripheral collisions at higher energy, the narrow vs wide peak sometimes becomes ambiguous.

$$v_n^2\{2\} = \frac{\sum_i (y_i - \delta_i) \frac{dN_i}{d\Delta\varphi_i}}{\sum_i \frac{dN_i}{d\Delta\varphi_i}}$$



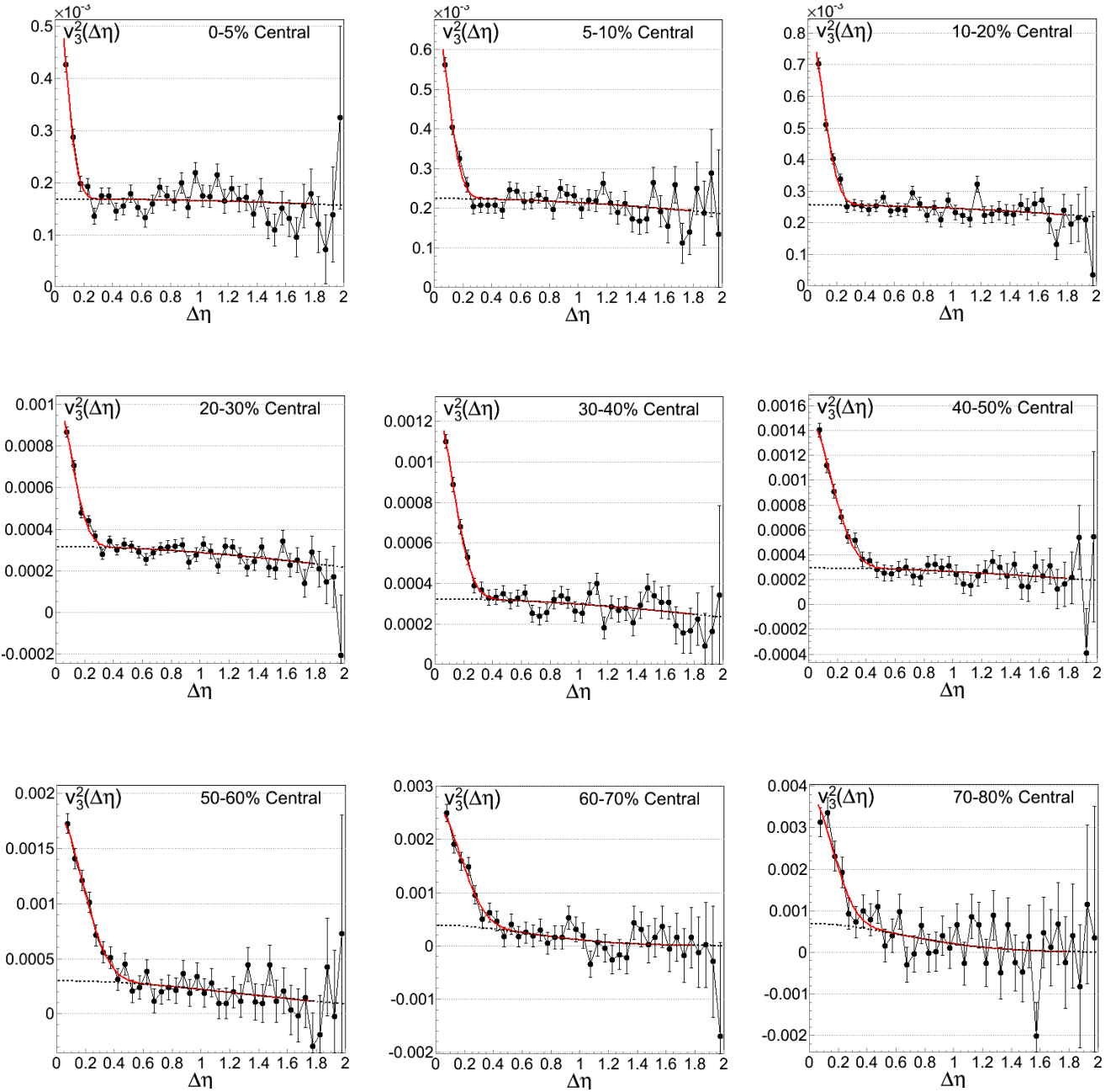
200 GeV Fits

all p_T



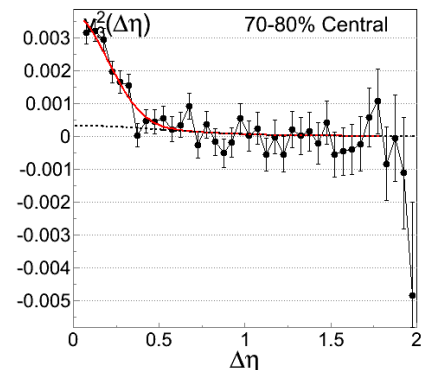
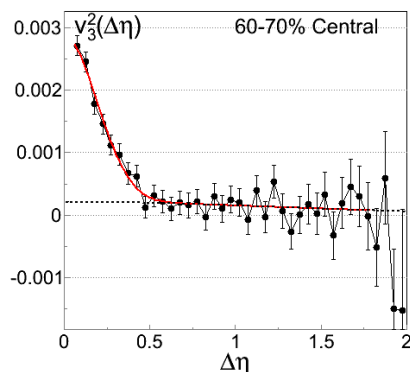
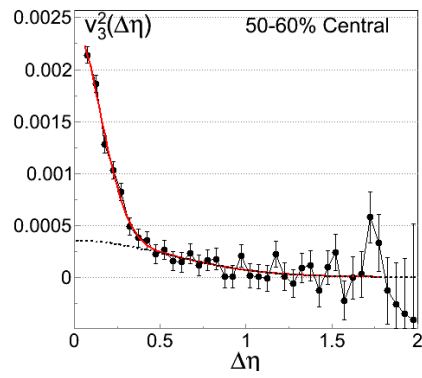
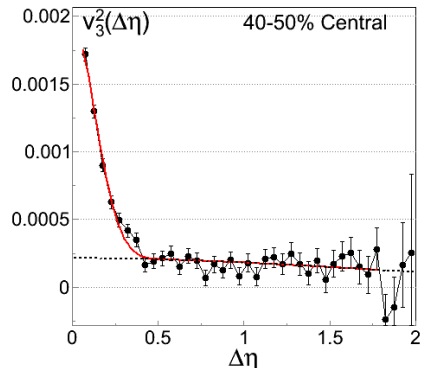
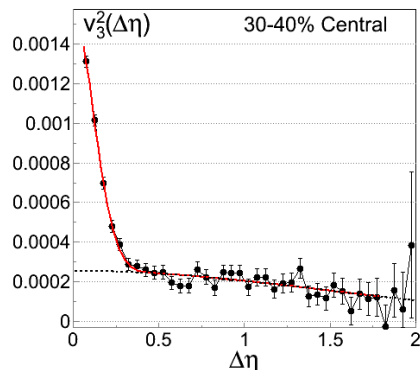
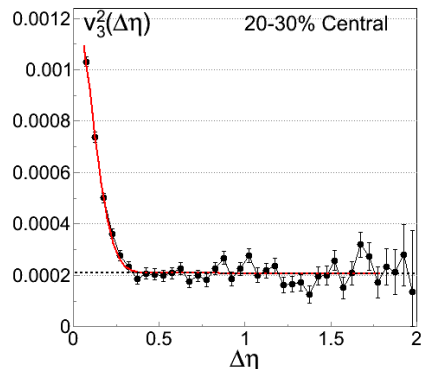
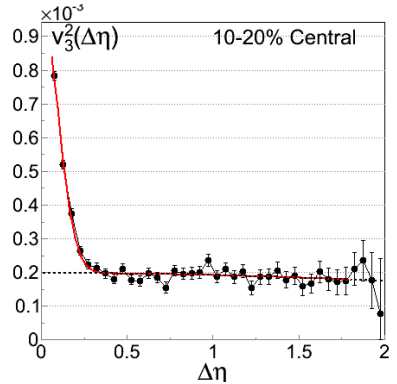
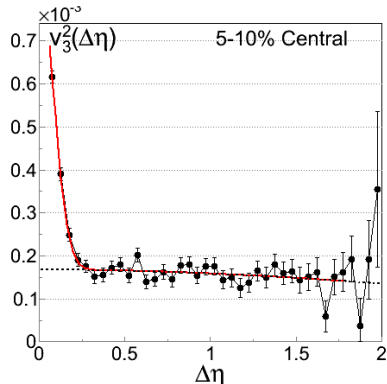
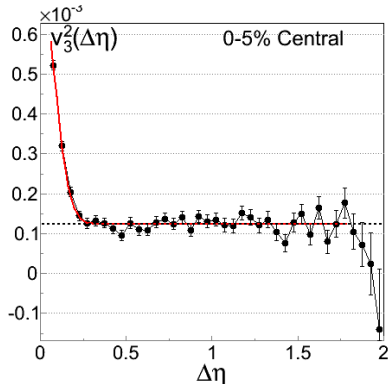
62.4 GeV Fits

all p_T



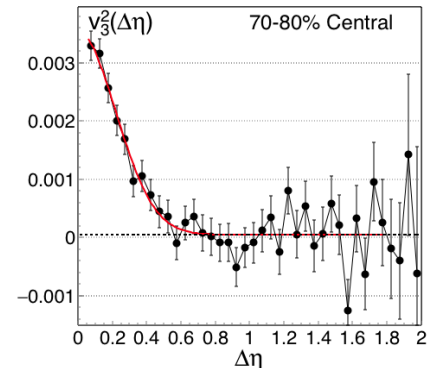
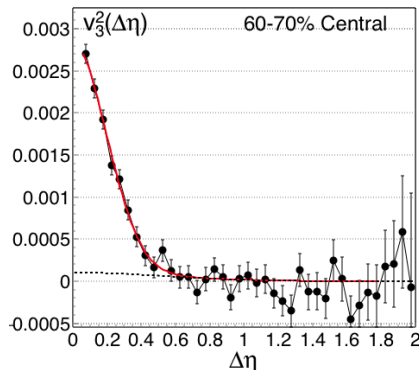
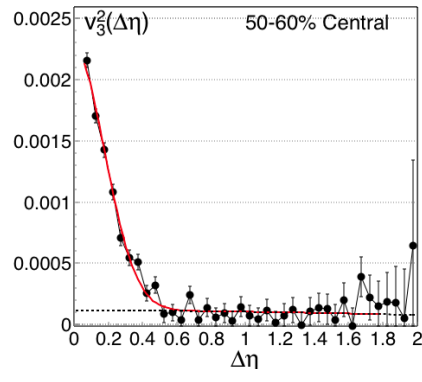
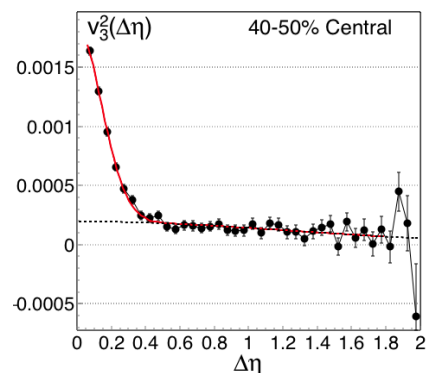
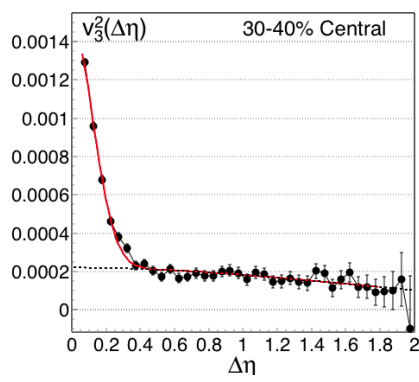
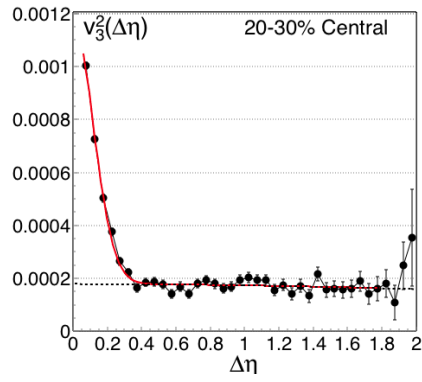
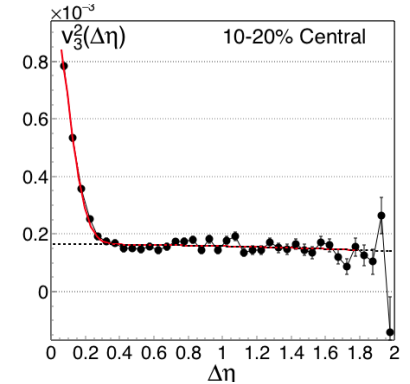
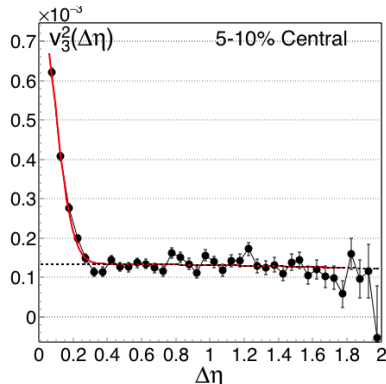
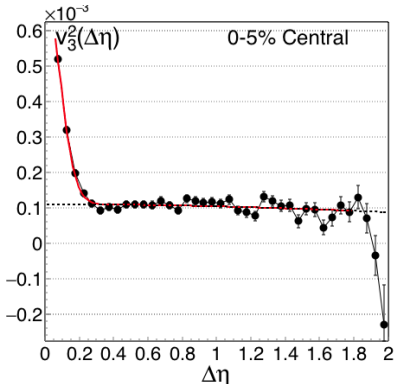
39 GeV Fits

all p_T



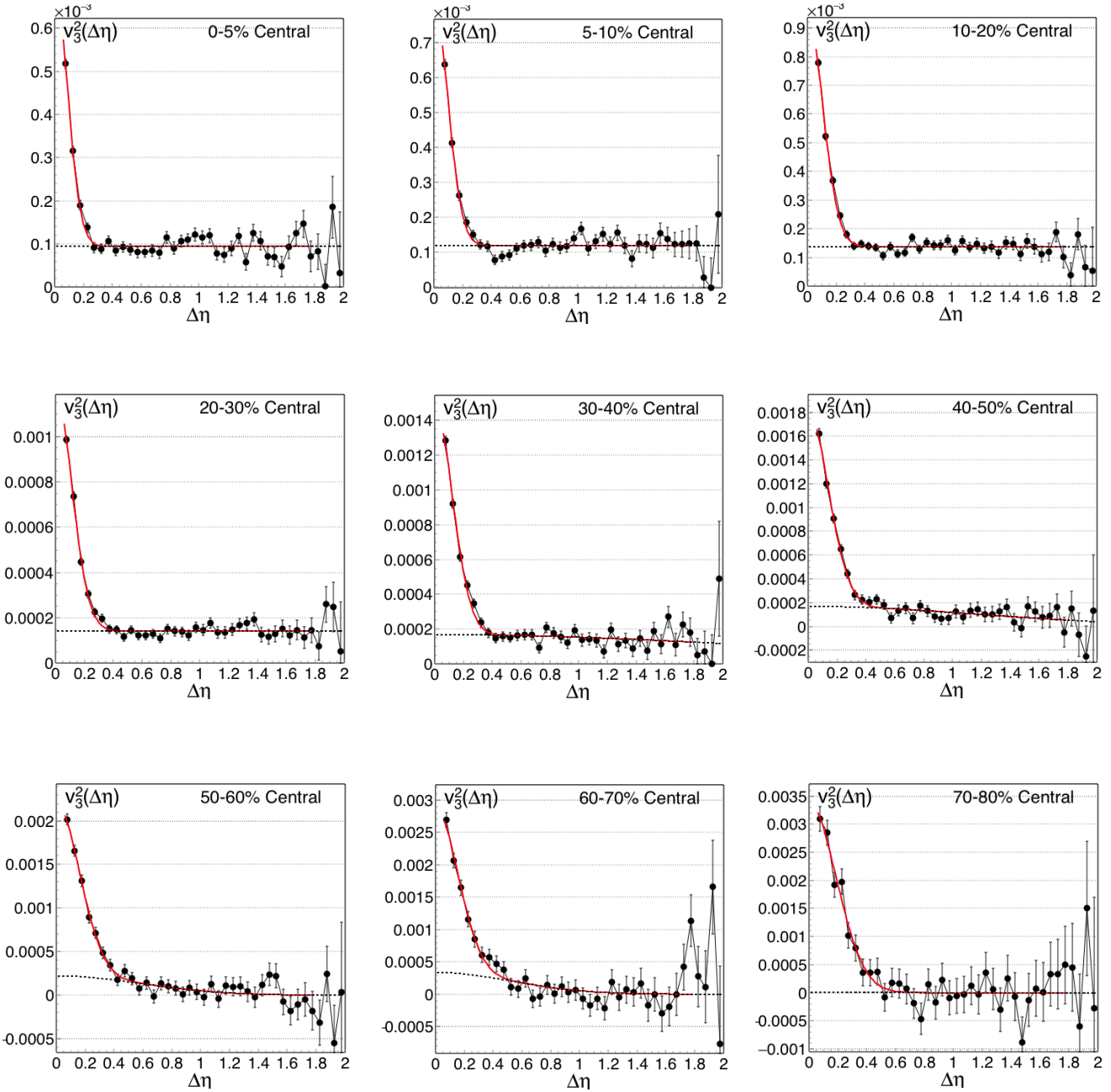
27 GeV Fits

all p_T



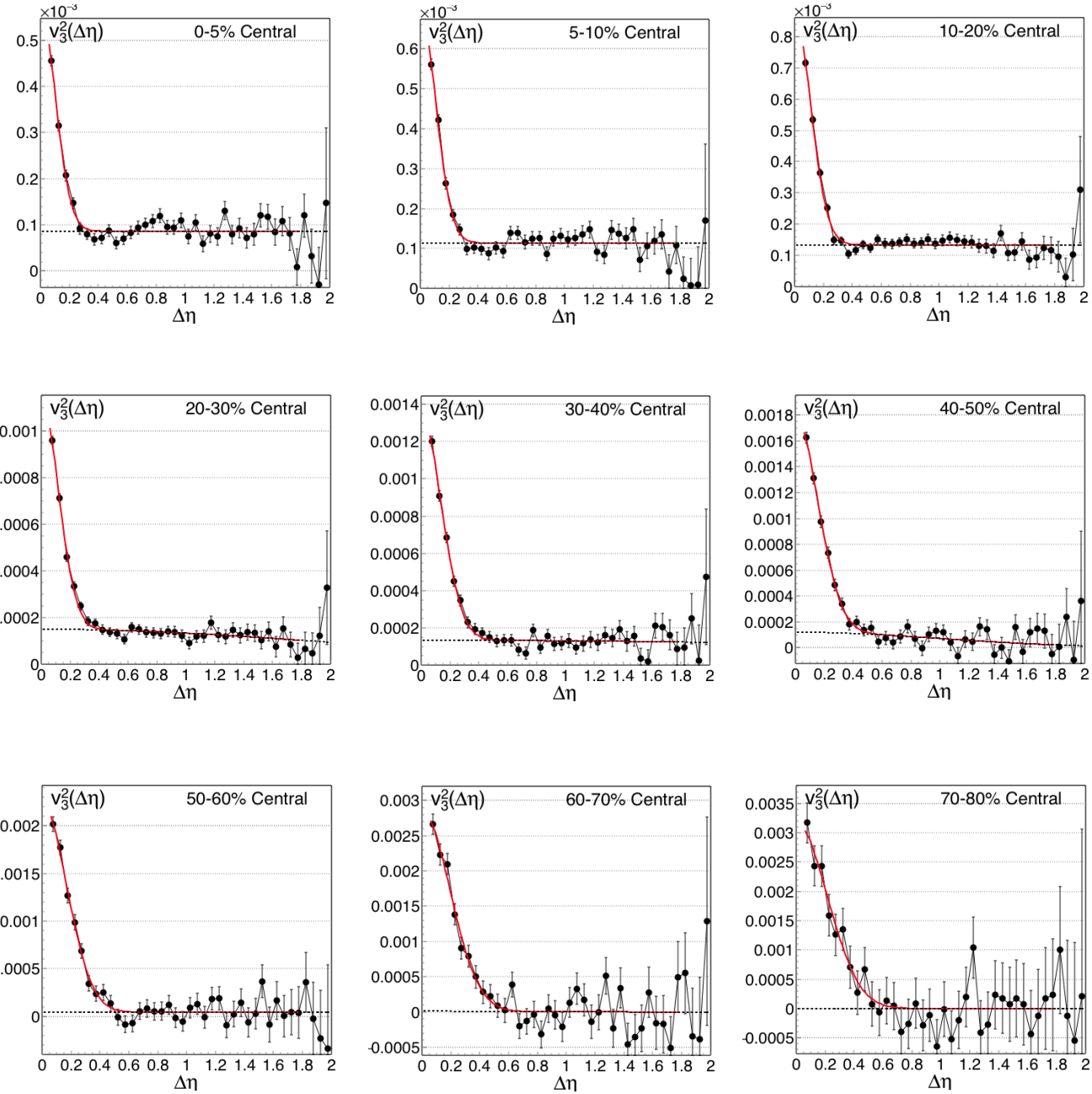
19.6 GeV Fits

all p_T



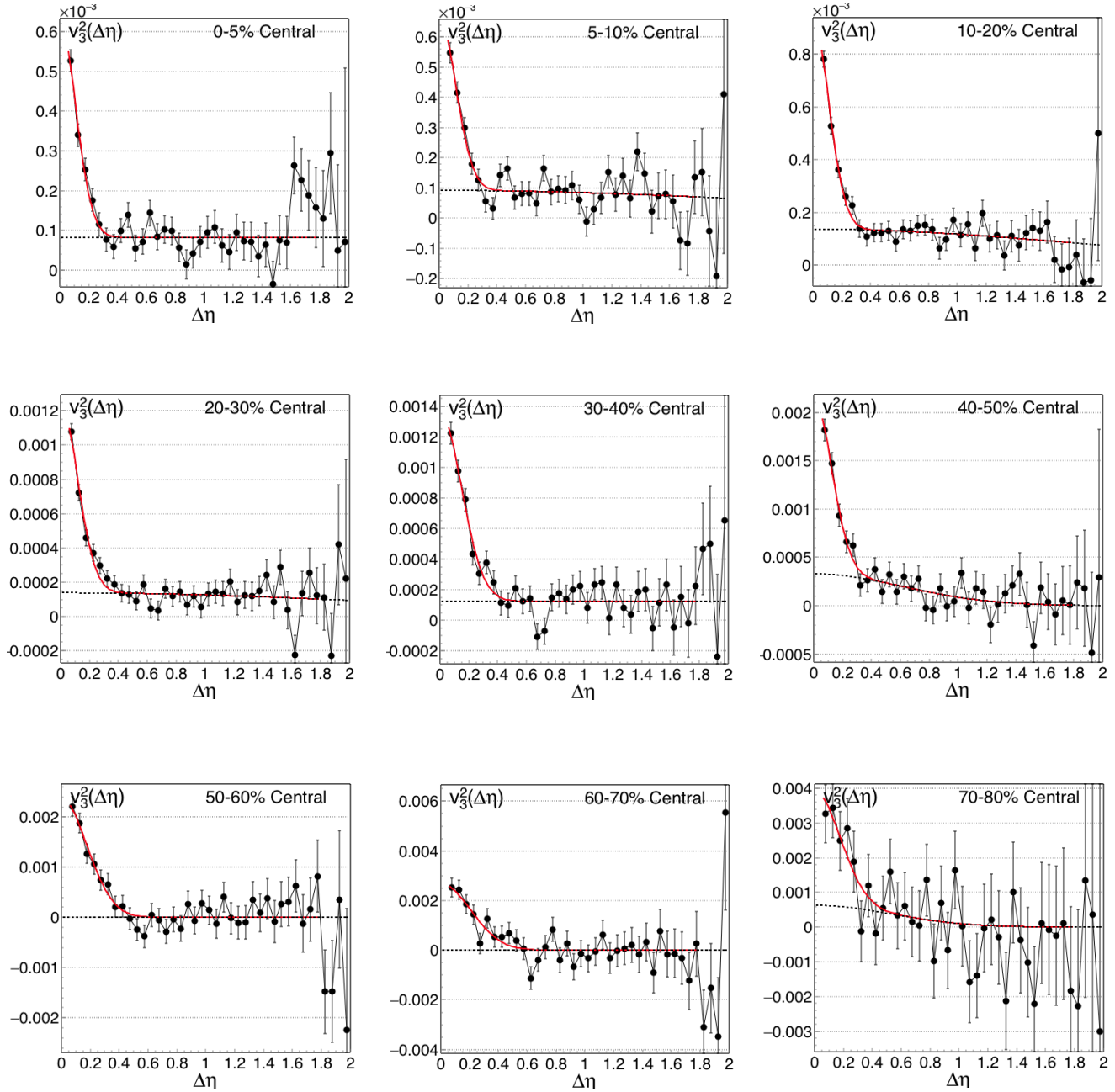
14.5 GeV Fits

all p_T



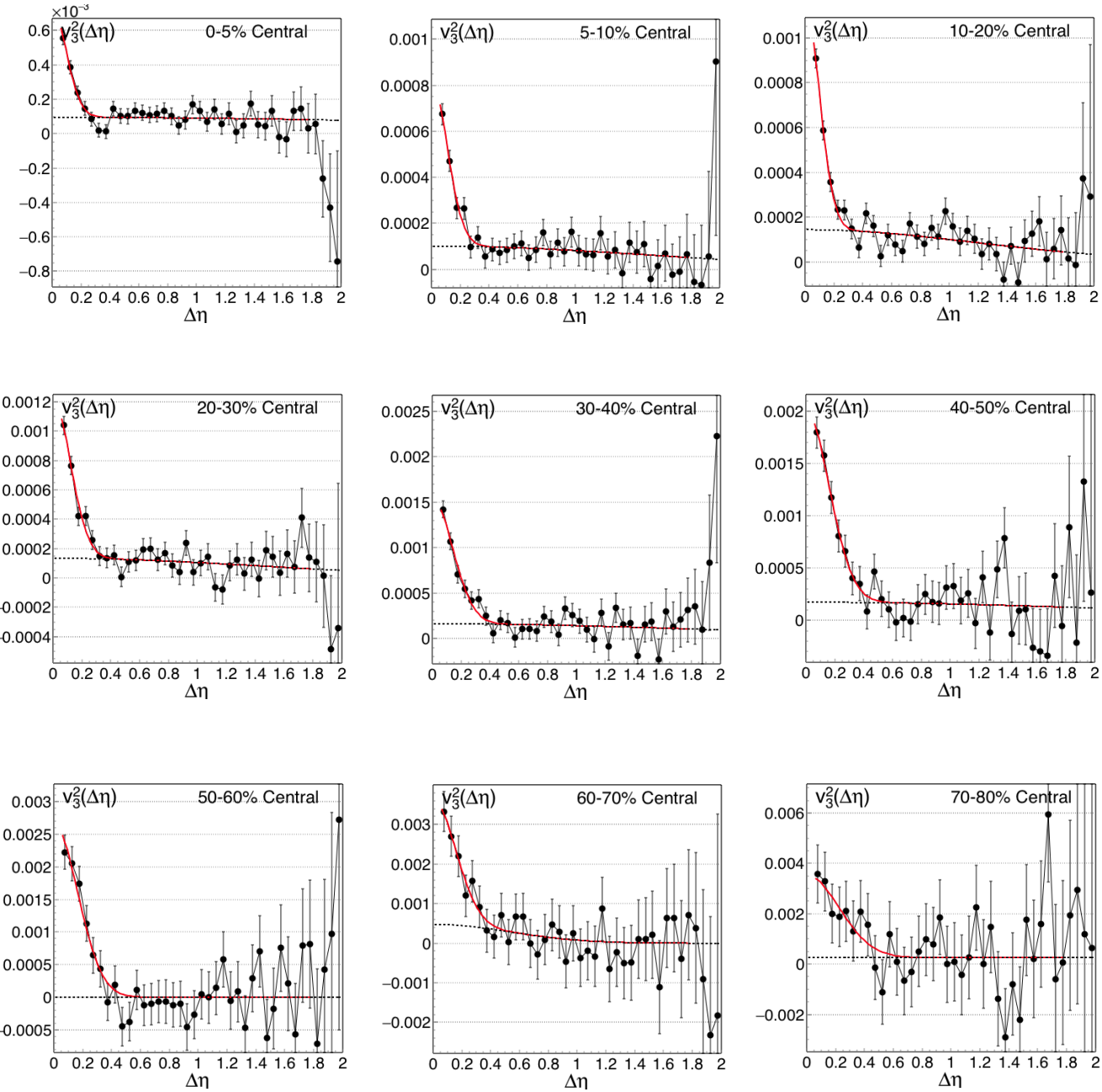
11.5 GeV Fits

all p_T



7.7 GeV Fits

all p_T



Systematic Uncertainty Estimates:

We checked the systematic uncertainties of our results by comparing run 4 with run 11, by changing the DCA cut from 3 to 2 cm, by comparing events with different z-vertex positions, by checking early parts of the run with late parts of the run, by using a high estimate for the efficiency vs a low estimate, and by comparing events where there were different numbers of bad RDO boards in the TPC. Our strategy is to compare all these checks to the standard analysis and use the largest result and lowest result as the upper and lower edge of the systematic error bands.

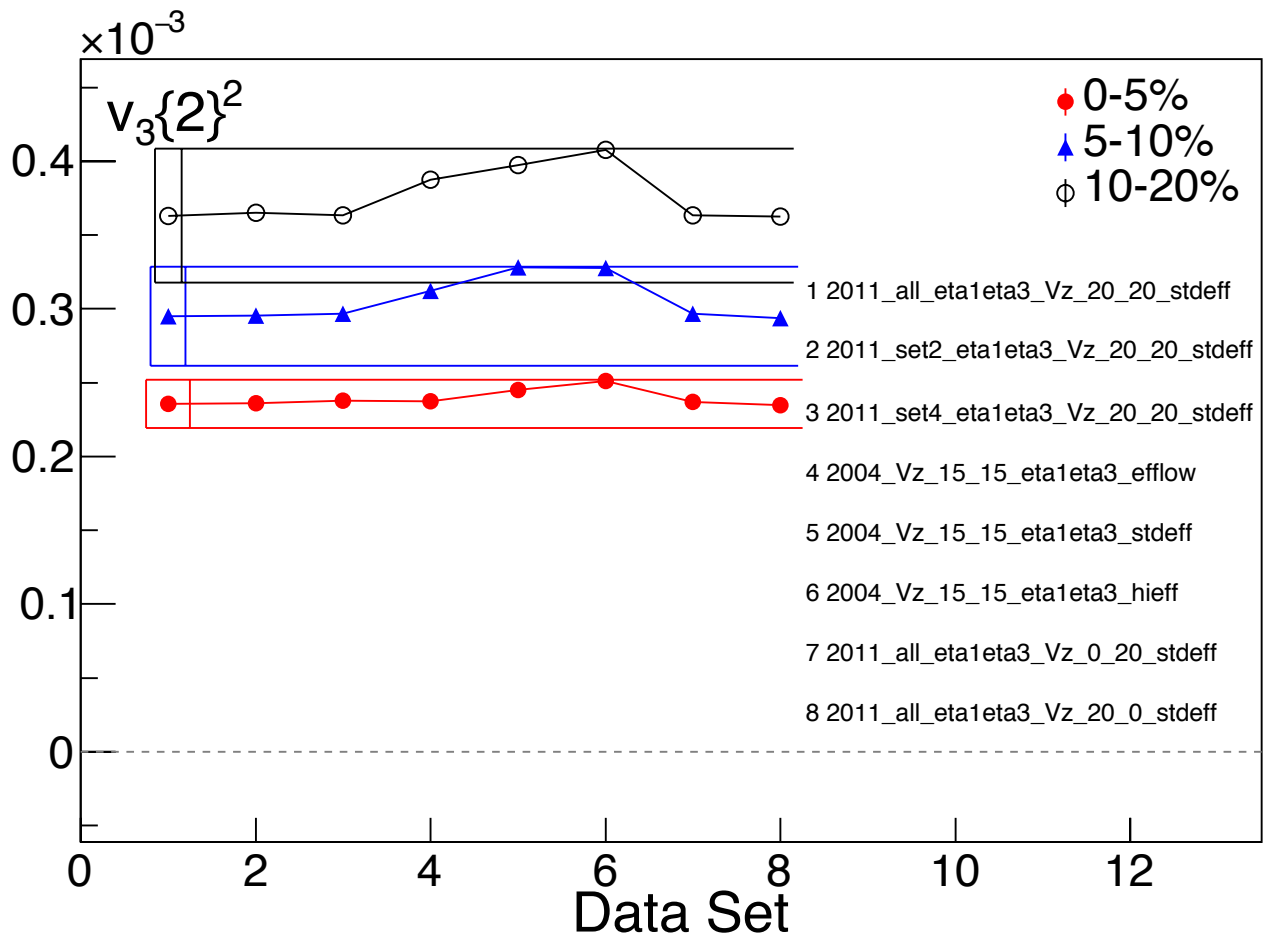
We also assign an error that is 10% of the residual corrections $\langle \cos 3\phi \rangle^2 + \langle \sin 3\phi \rangle^2$. As mentioned before, this correction is very small so this is not a big contributing factor. We also assign an uncertainty on the subtraction of the HBT peak which is 10% of the estimated contribution of the peak to the total correlation function. This amounts to assuming that we may have over or under-estimated the contribution from the HBT peak by about 10%.

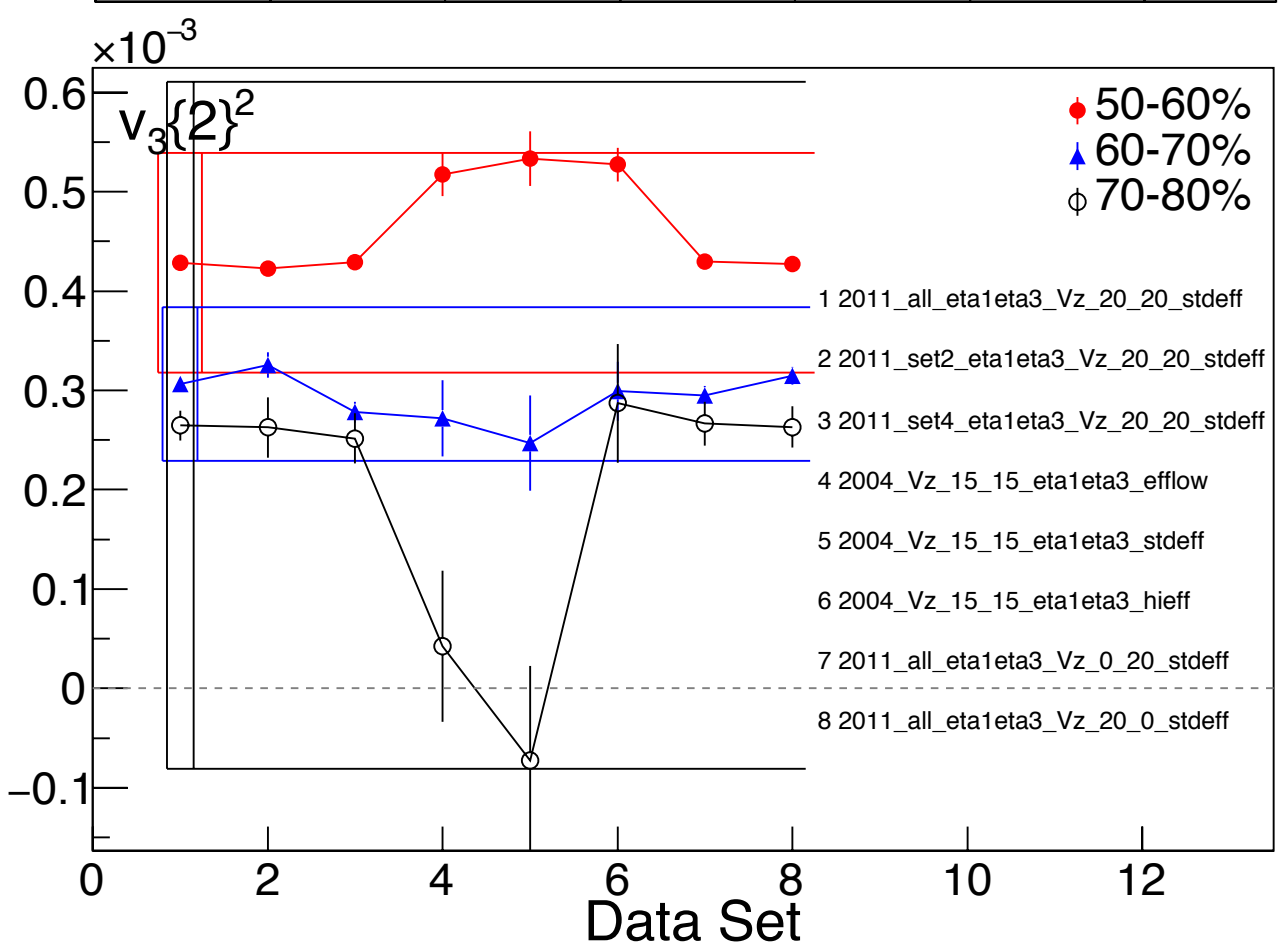
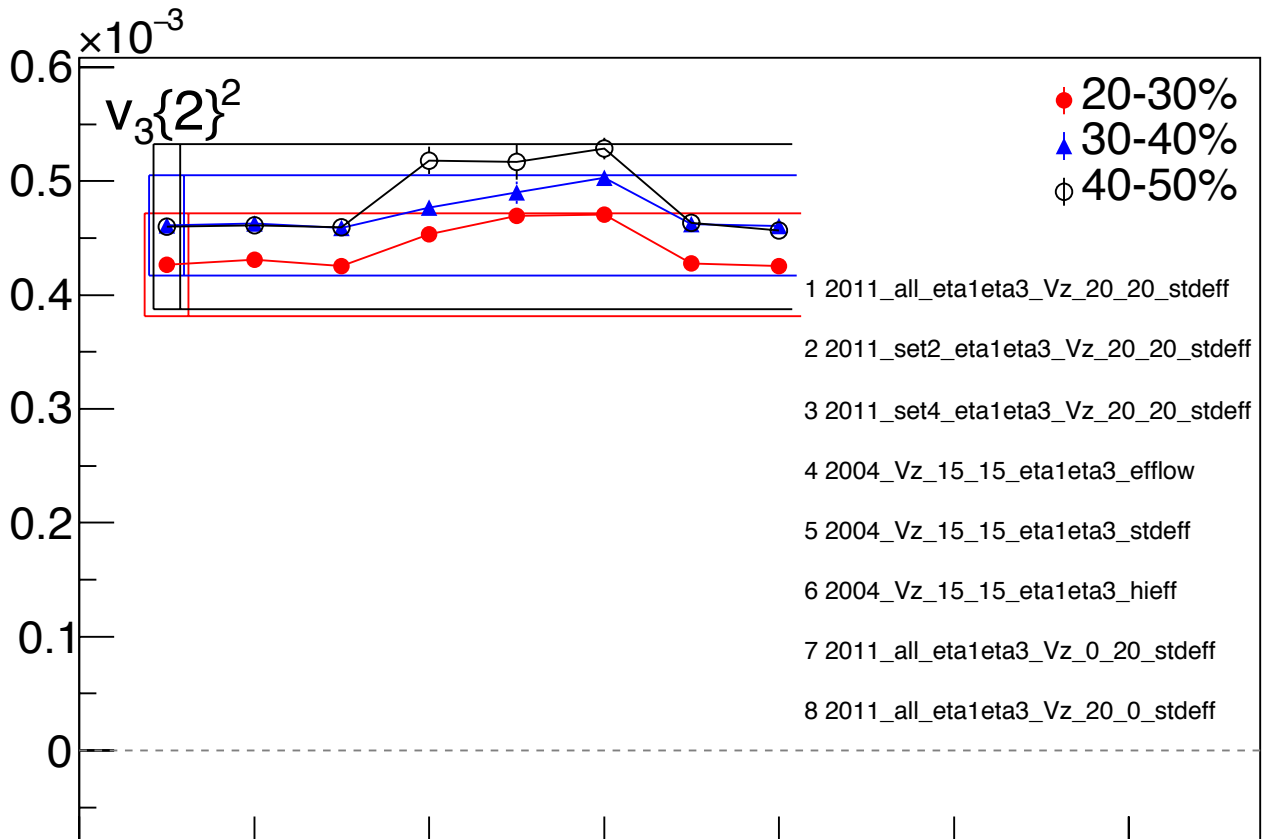
We have decided to exclude the positive z-vertex vs negative z-vertex from the final systematic error calculation. We've found that because those two are statistically independent of each other, the differences between them seem to be more related to statistical fluctuations than a systematic difference. Including that spread in the final calculation would simply double count the statistical errors. The updated plots reflect the smaller systematic errors. We assume the systematic errors are symmetric. As an example of our reasoning, if changing the DCA from 3 to 2 causes the result to go one way, then it's a good assumption that if we had changed it from 3 to 4 it would have gone the other way.

The final systematic errors are generated by adding all errors in quadrature. We present in the following several studies along with trend plots that show the final errors for each energy and centrality. The $Vz > 0$ and $Vz < 0$ data are shown on the trend plots but are not part of the final calculation.

Systematic Uncertainty Estimates 200 GeV:

The 200 GeV data shows a small 2004 vs 2011 deviation that is larger than all other variations. The number of dead RDO's did not contribute much to the errors. In the following plot "Data Set" represents a different analysis of the same observable either with a totally different data set or with different analysis procedures or cuts. Generally, the results appear to be very stable.

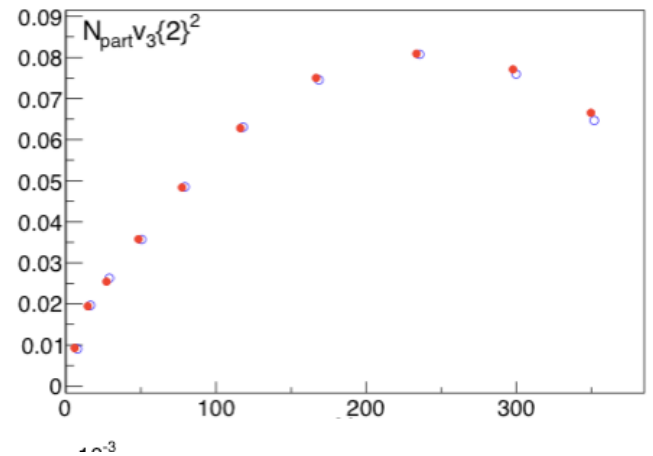
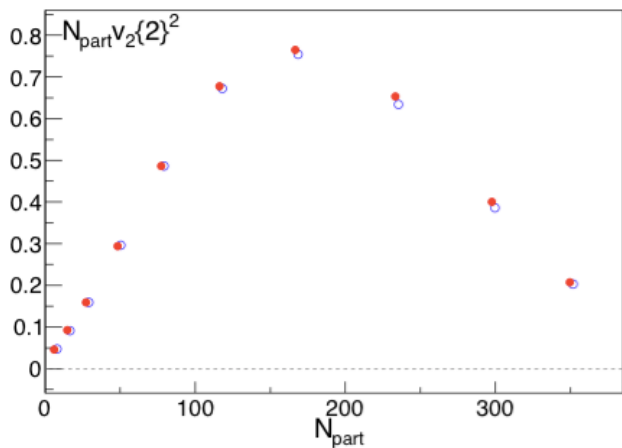




Systematic Uncertainty Estimates 200 GeV:

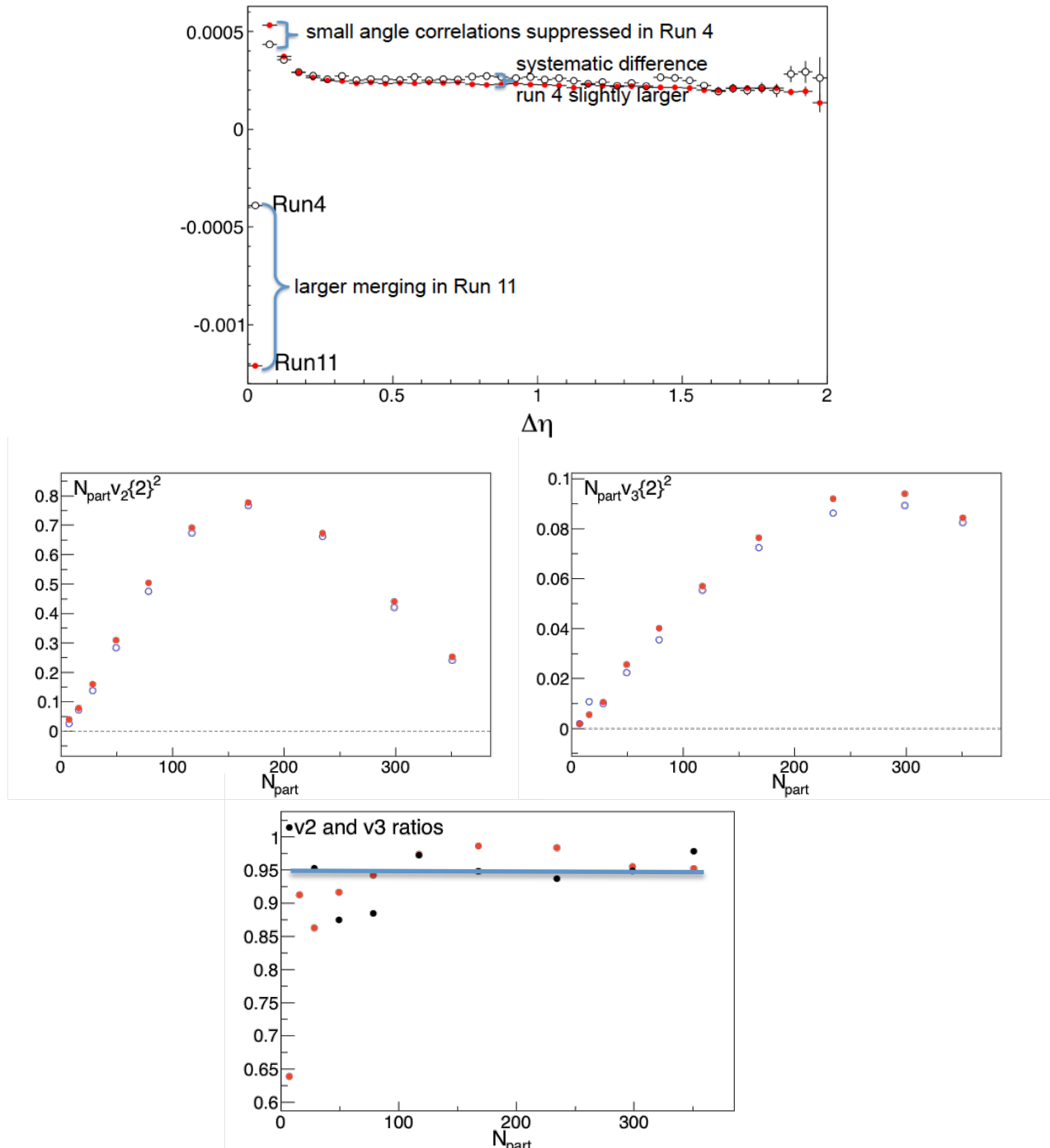
Here is a closer look at the change with the number of dead RDO's. Results are stable.

6 Dead RDO's vs 4 Dead RDO's



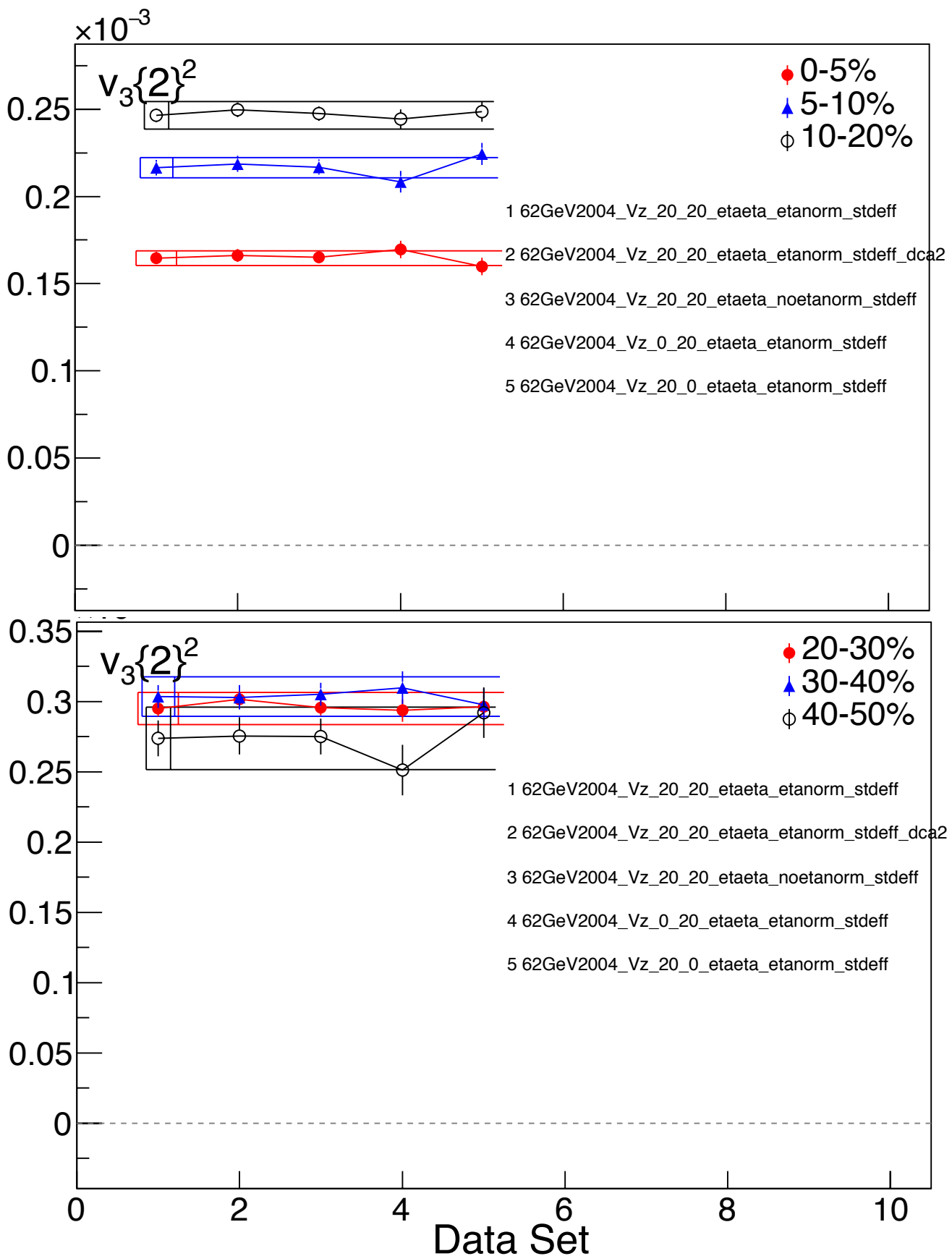
200 GeV A Closer Look at Run 4 vs Run 11:

Some residual differences between Run 11 and Run 4 couldn't be removed but they are much smaller than past differences and go in to our systematic error estimate.

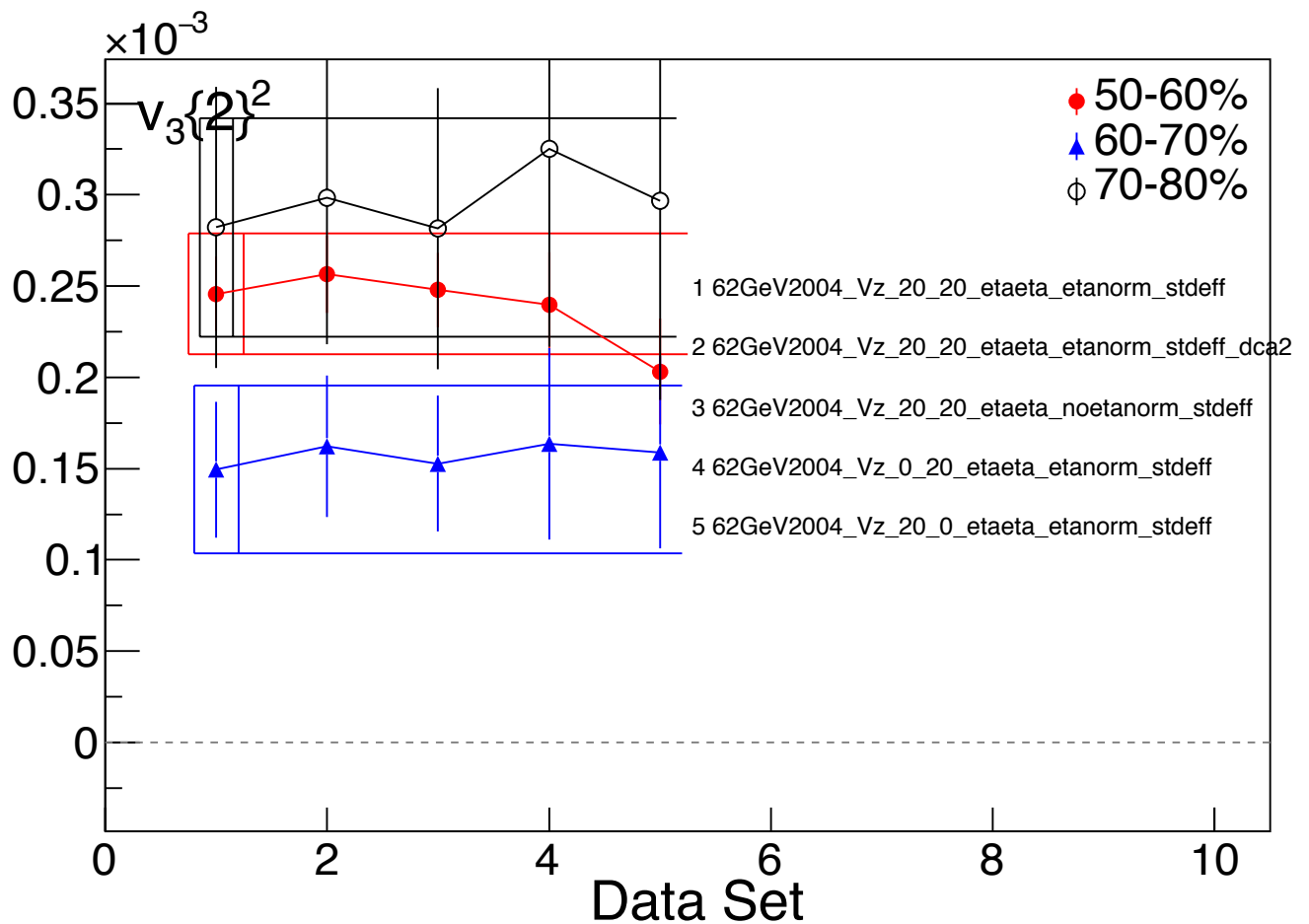


The residual deviation between Run 4 and Run 11 for v2 and v3 is 2.5% (5% on v_n^2).

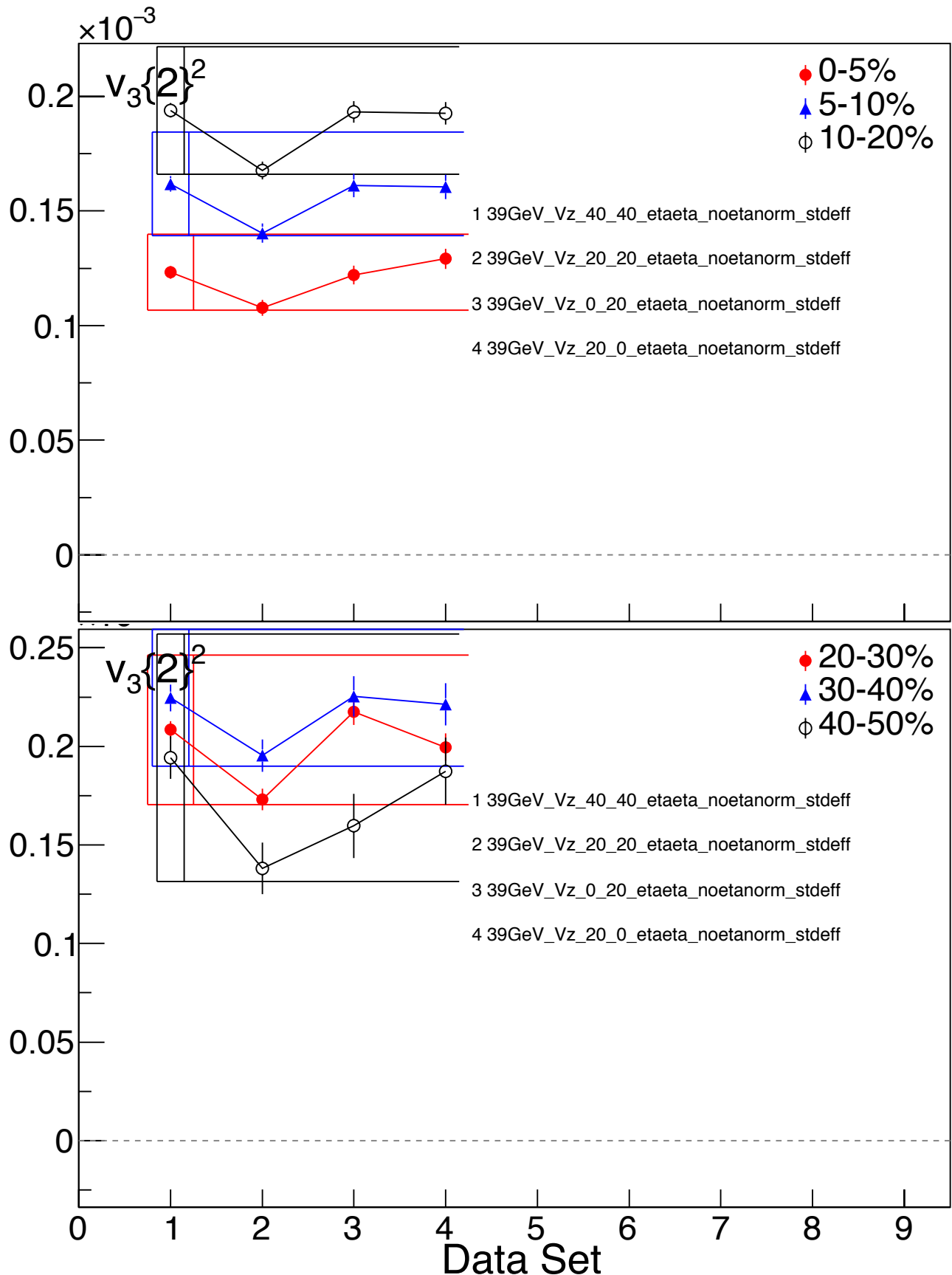
Systematic Uncertainty Estimates 62.4 GeV:



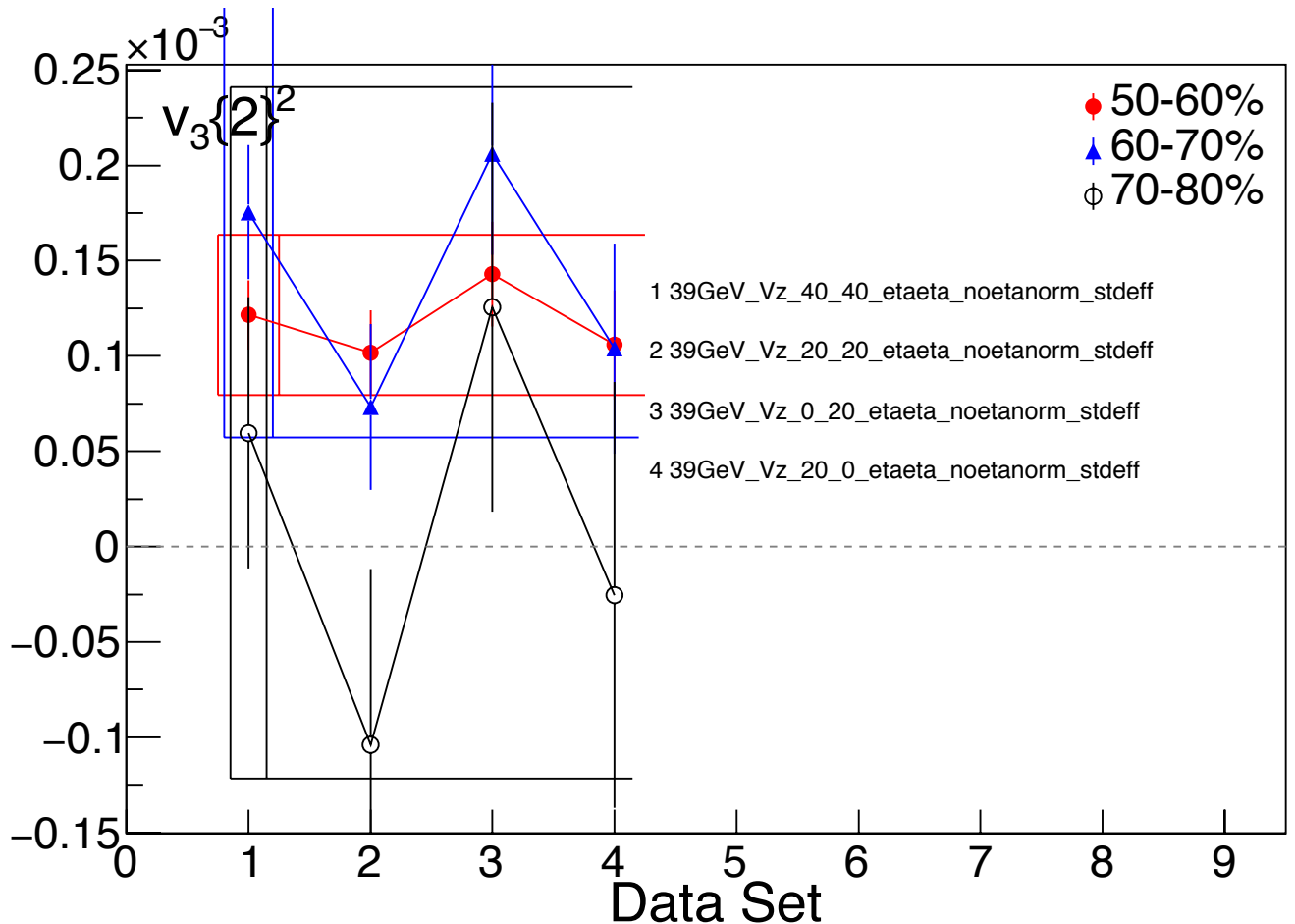
Systematic Uncertainty Estimates 62.4 GeV:



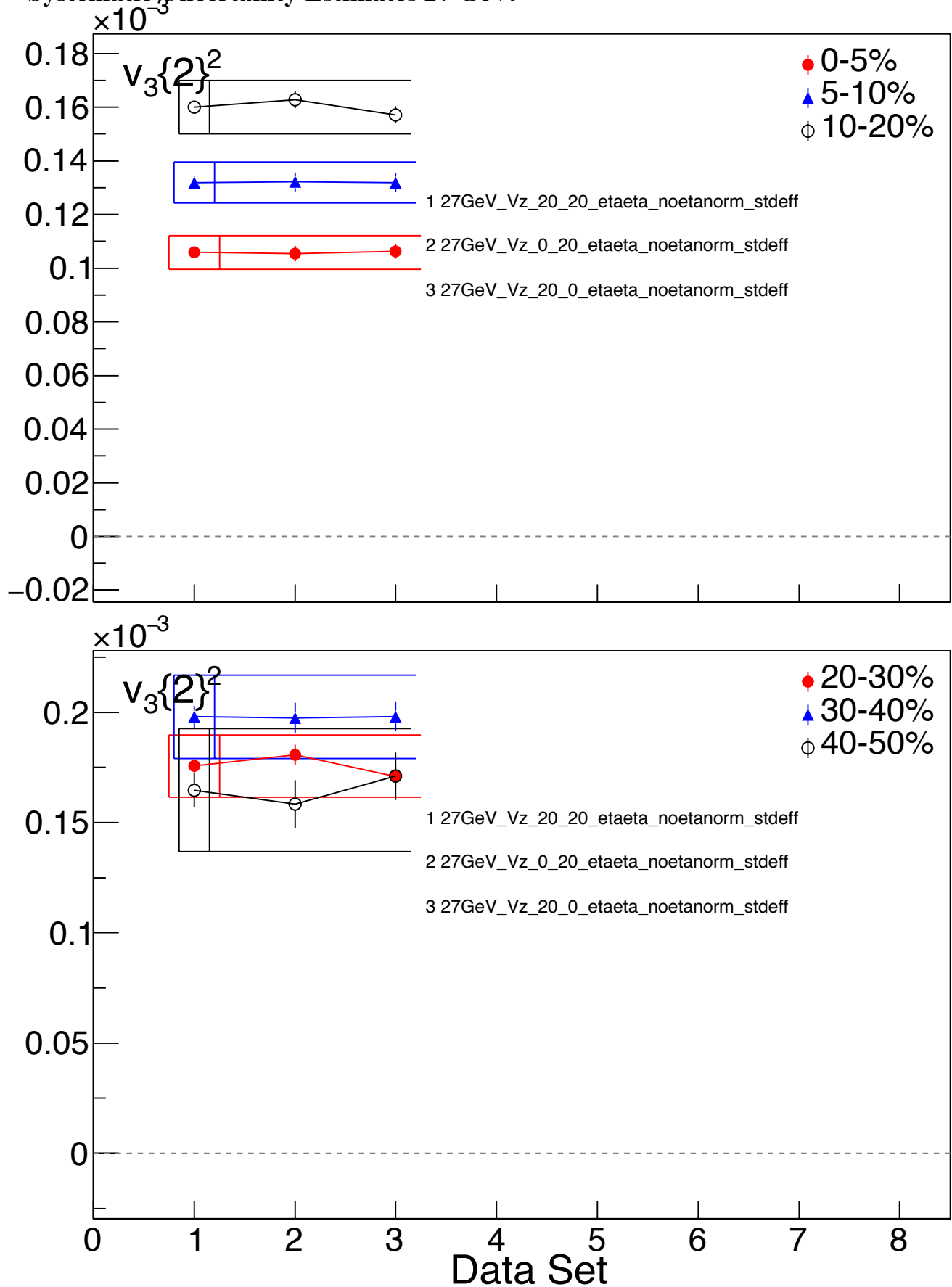
Systematic Uncertainty Estimates 39 GeV:



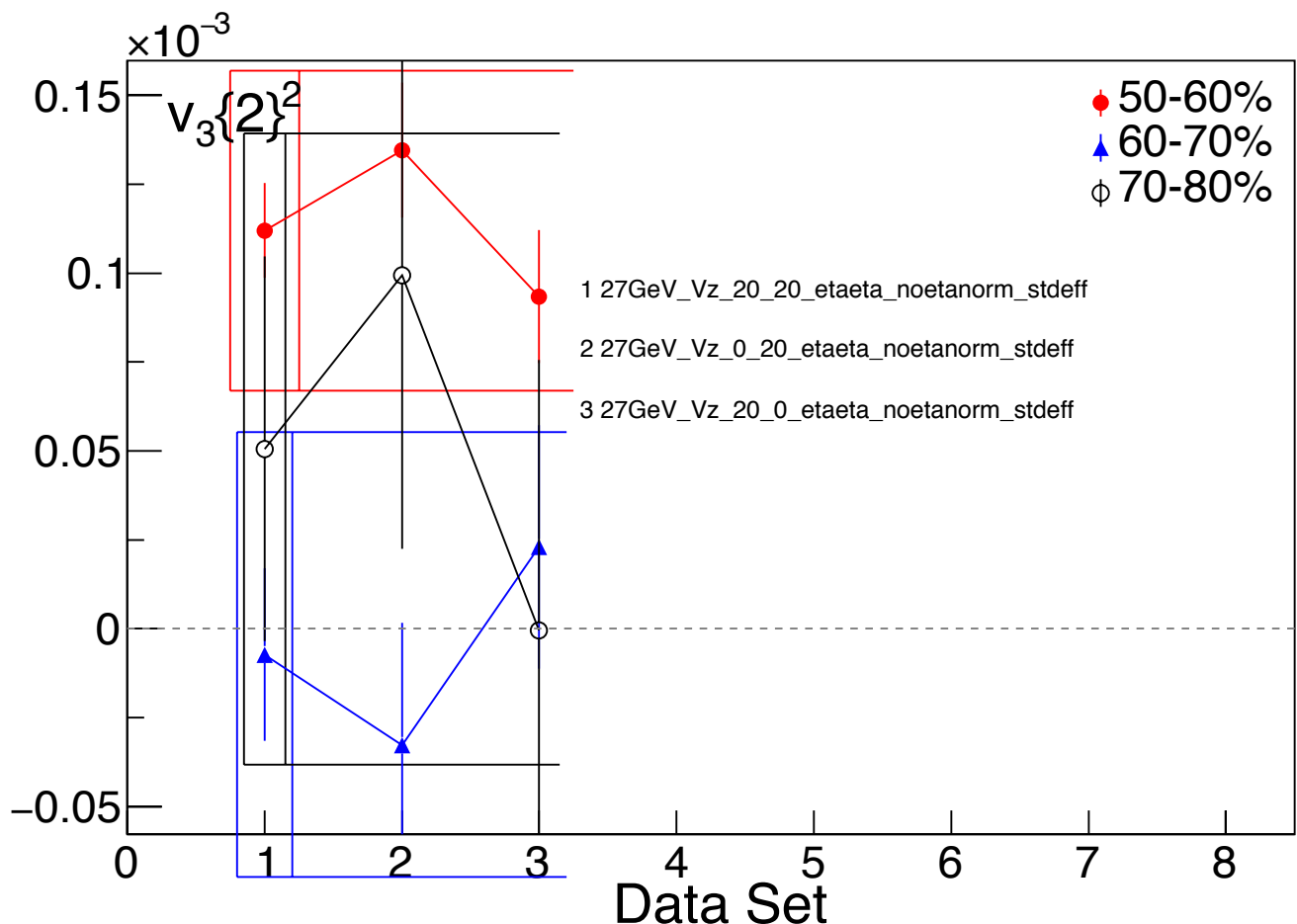
Systematic Uncertainty Estimates 39 GeV:



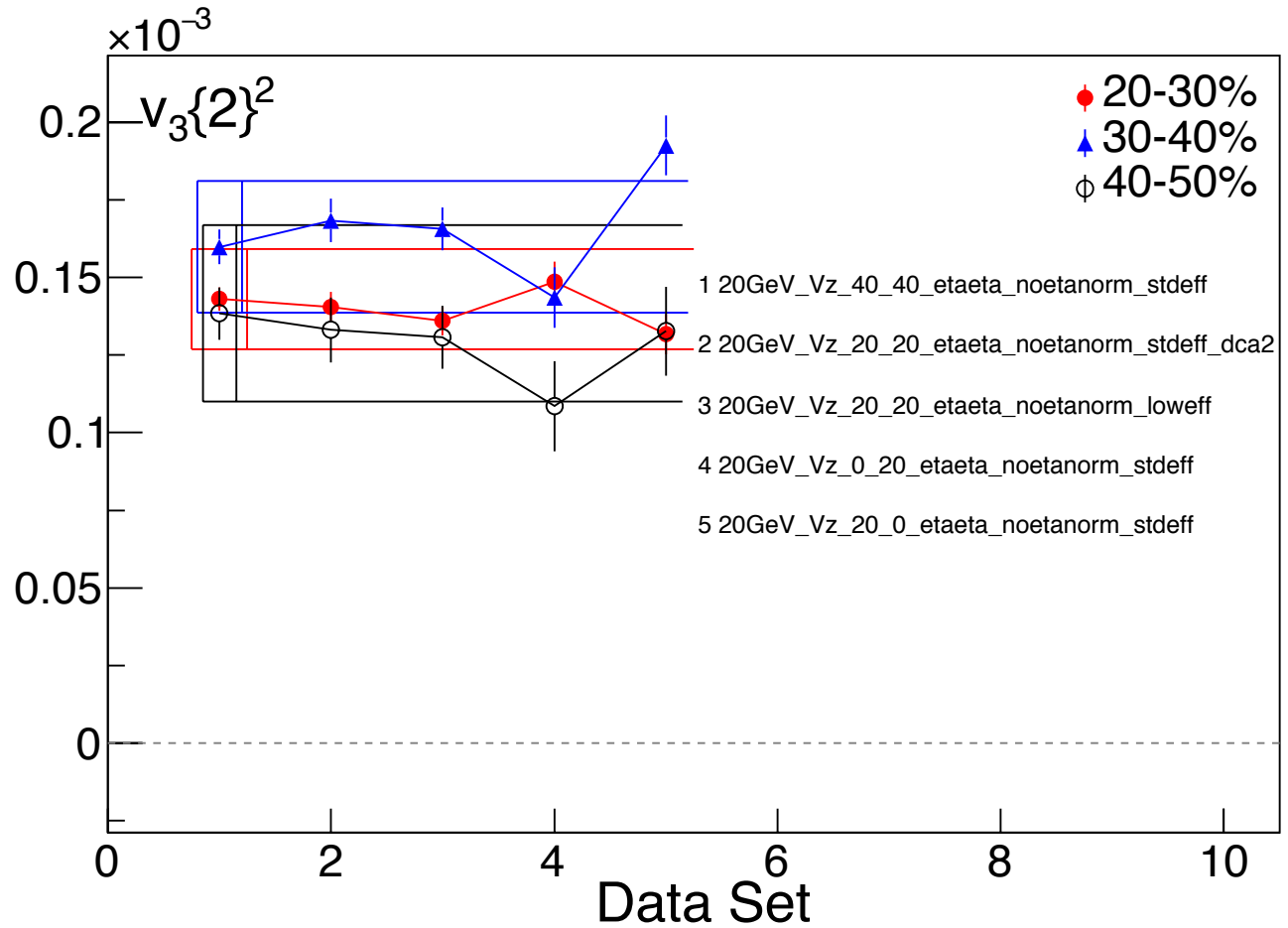
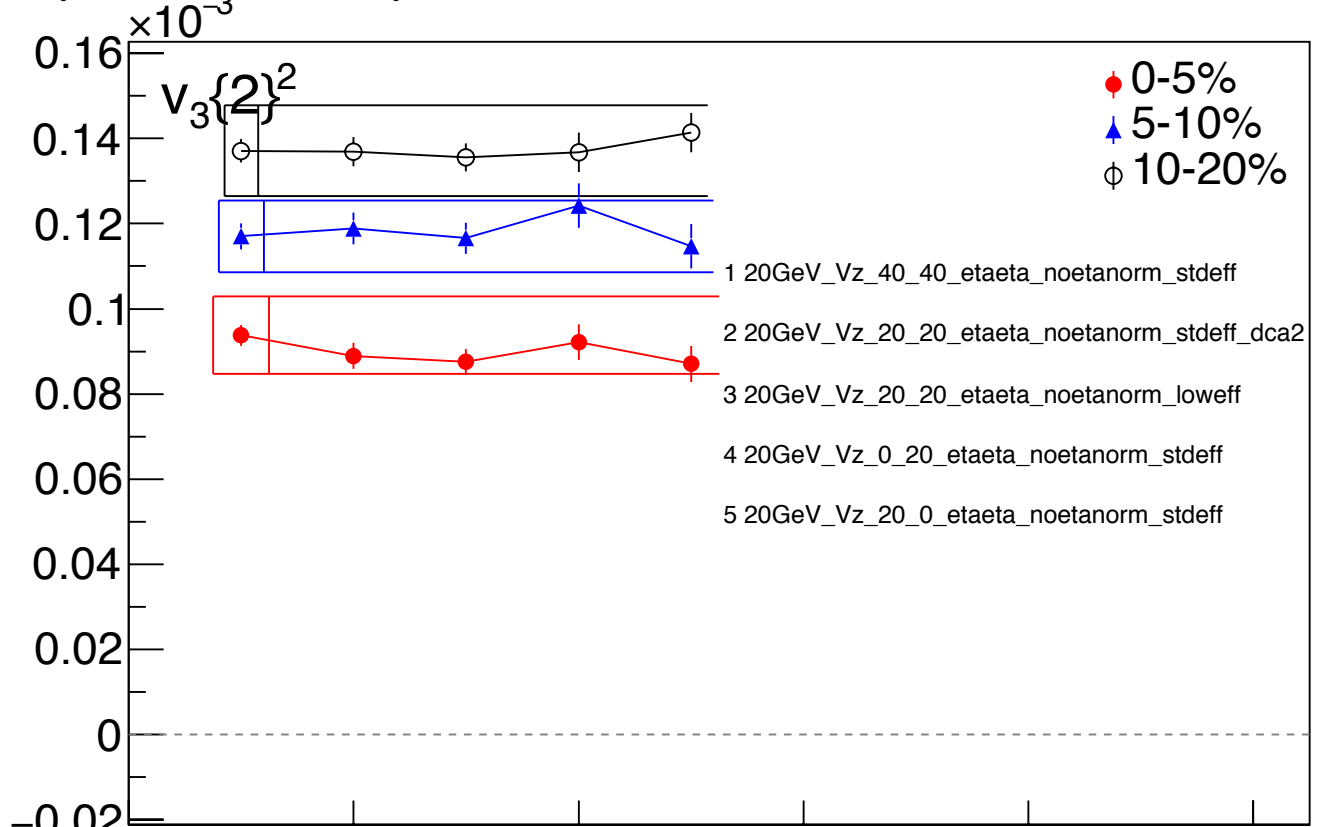
Systematic Uncertainty Estimates 27 GeV:



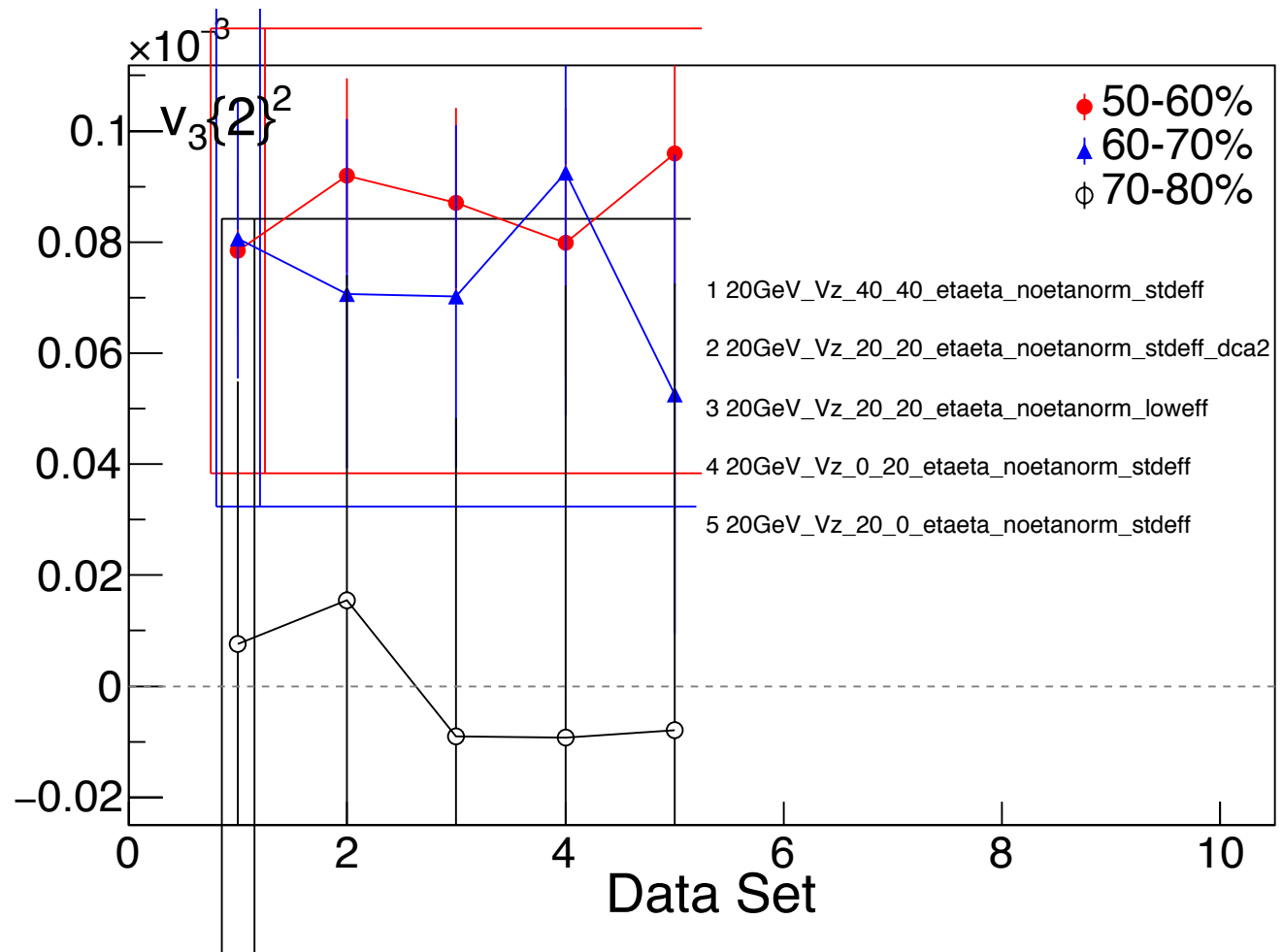
Systematic Uncertainty Estimates 27 GeV:



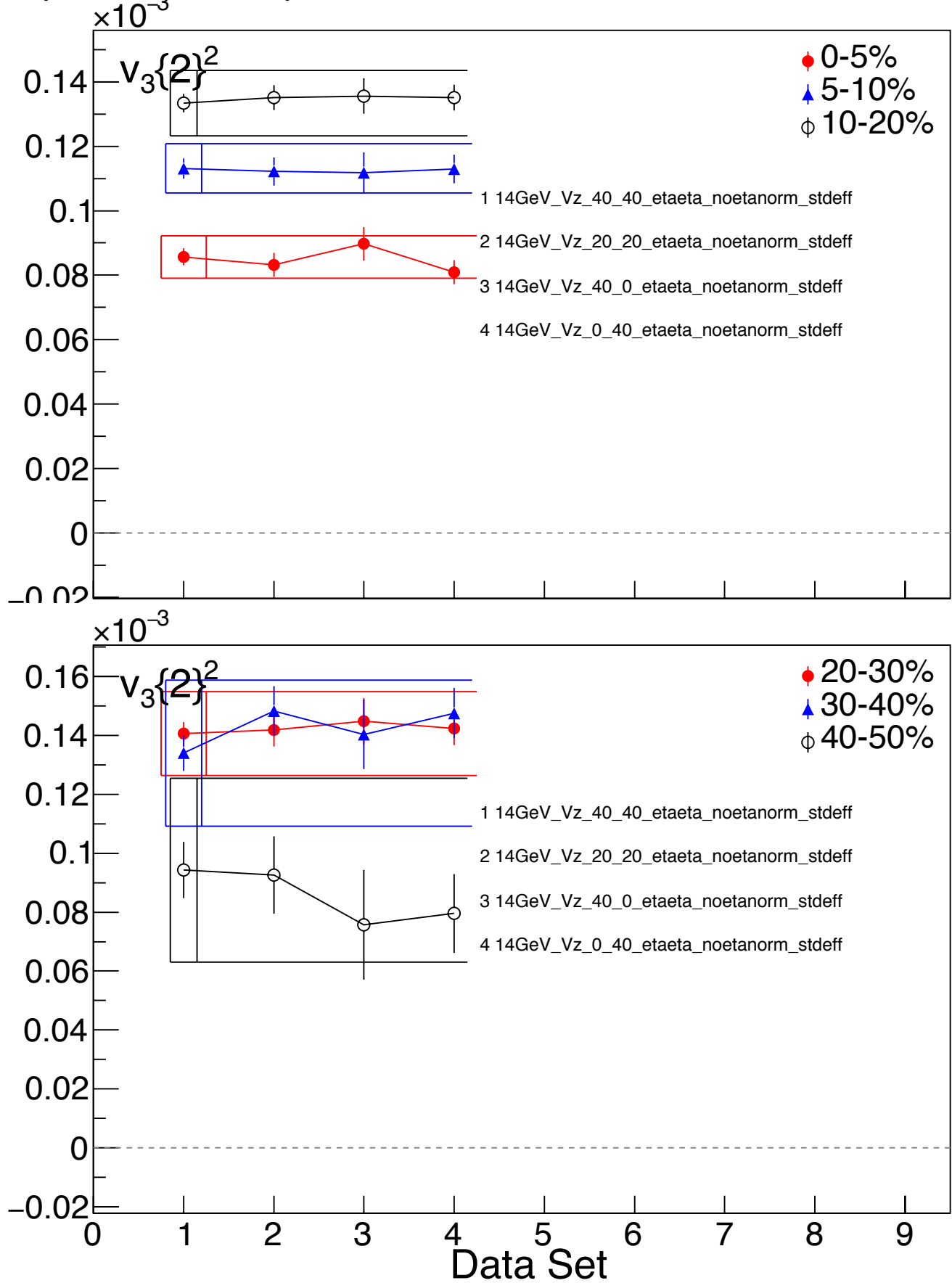
Systematic Uncertainty Estimates 19.6 GeV:



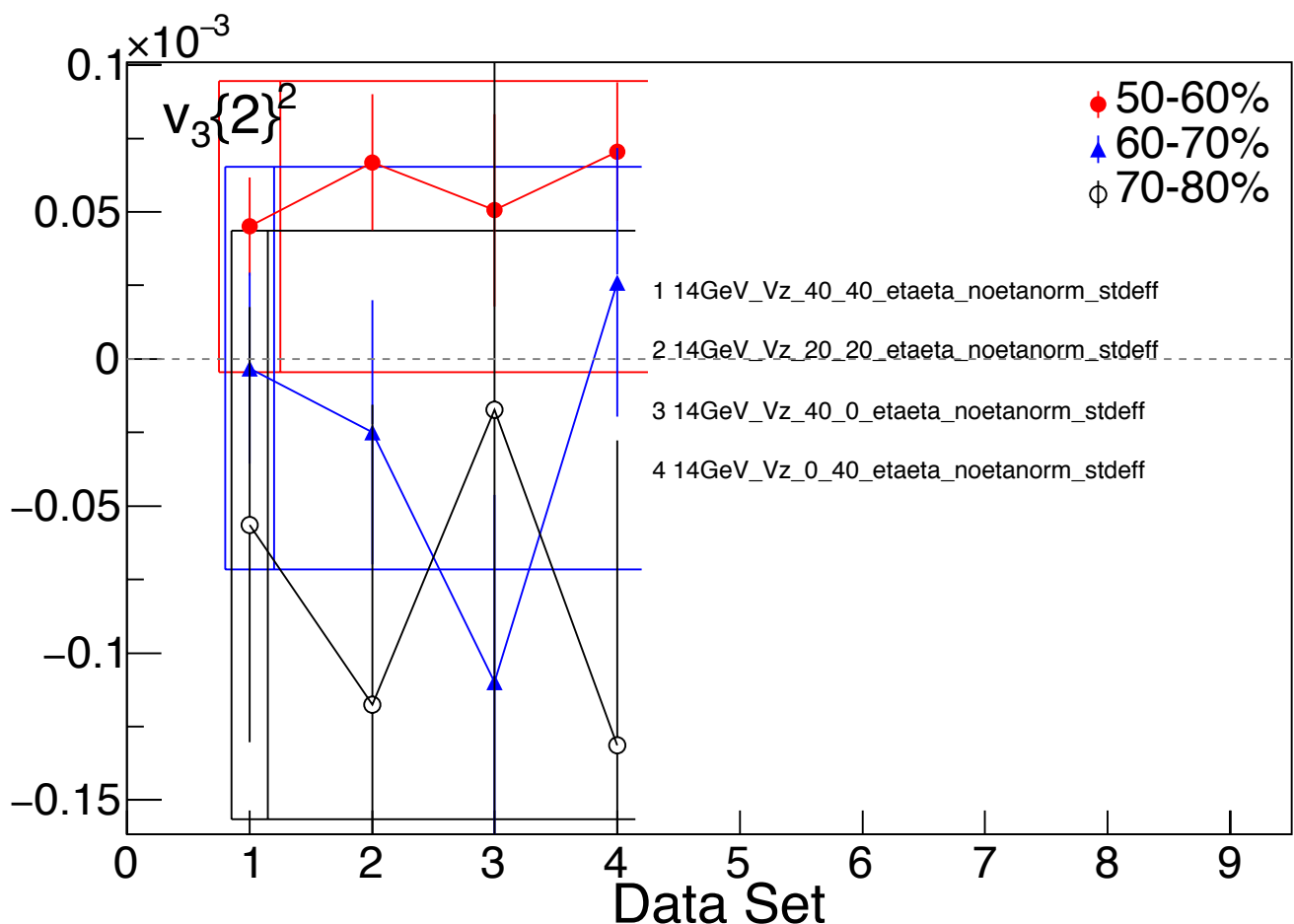
Systematic Uncertainty Estimates 19.6 GeV:



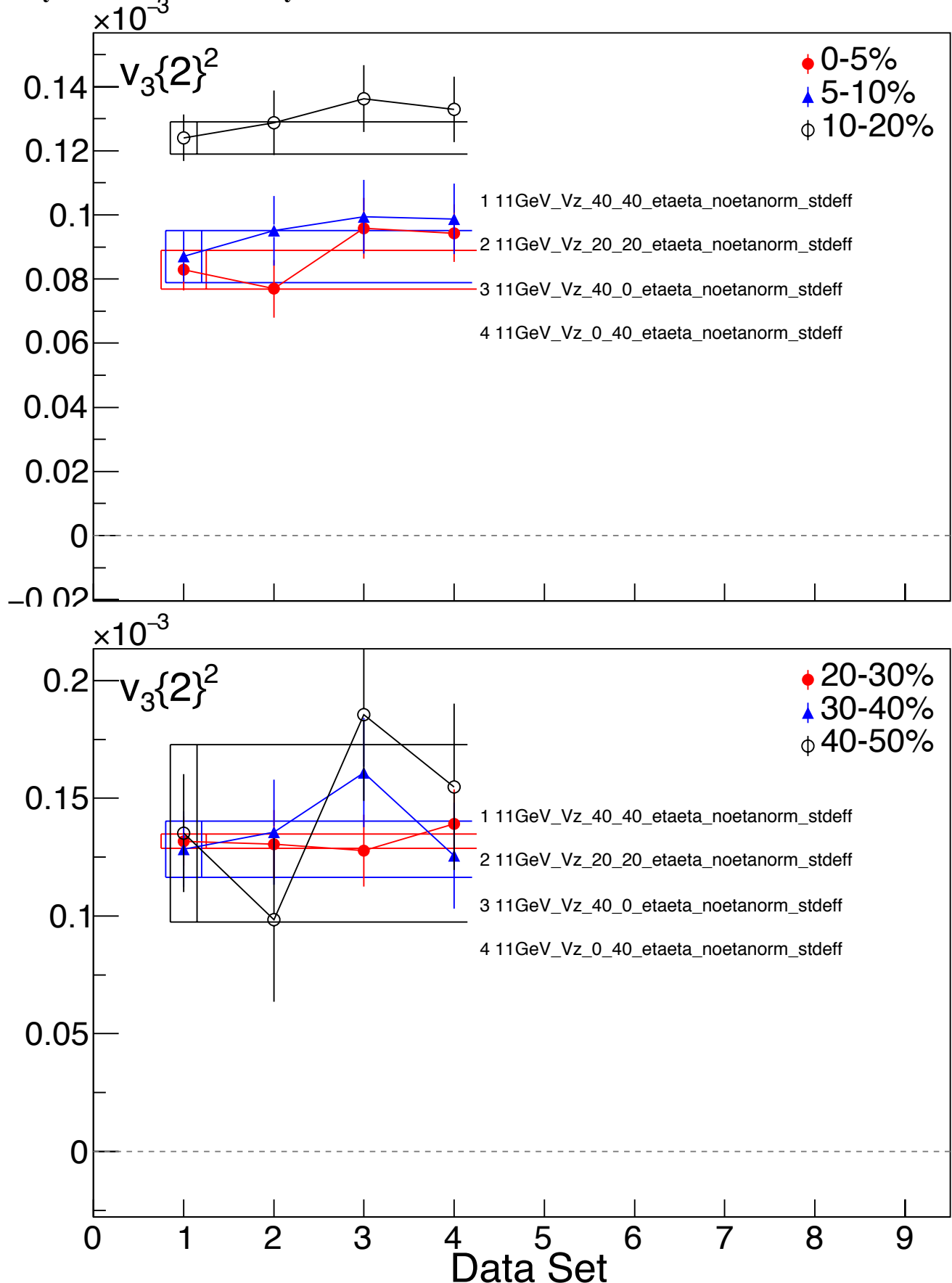
Systematic Uncertainty Estimates 14.5 GeV:



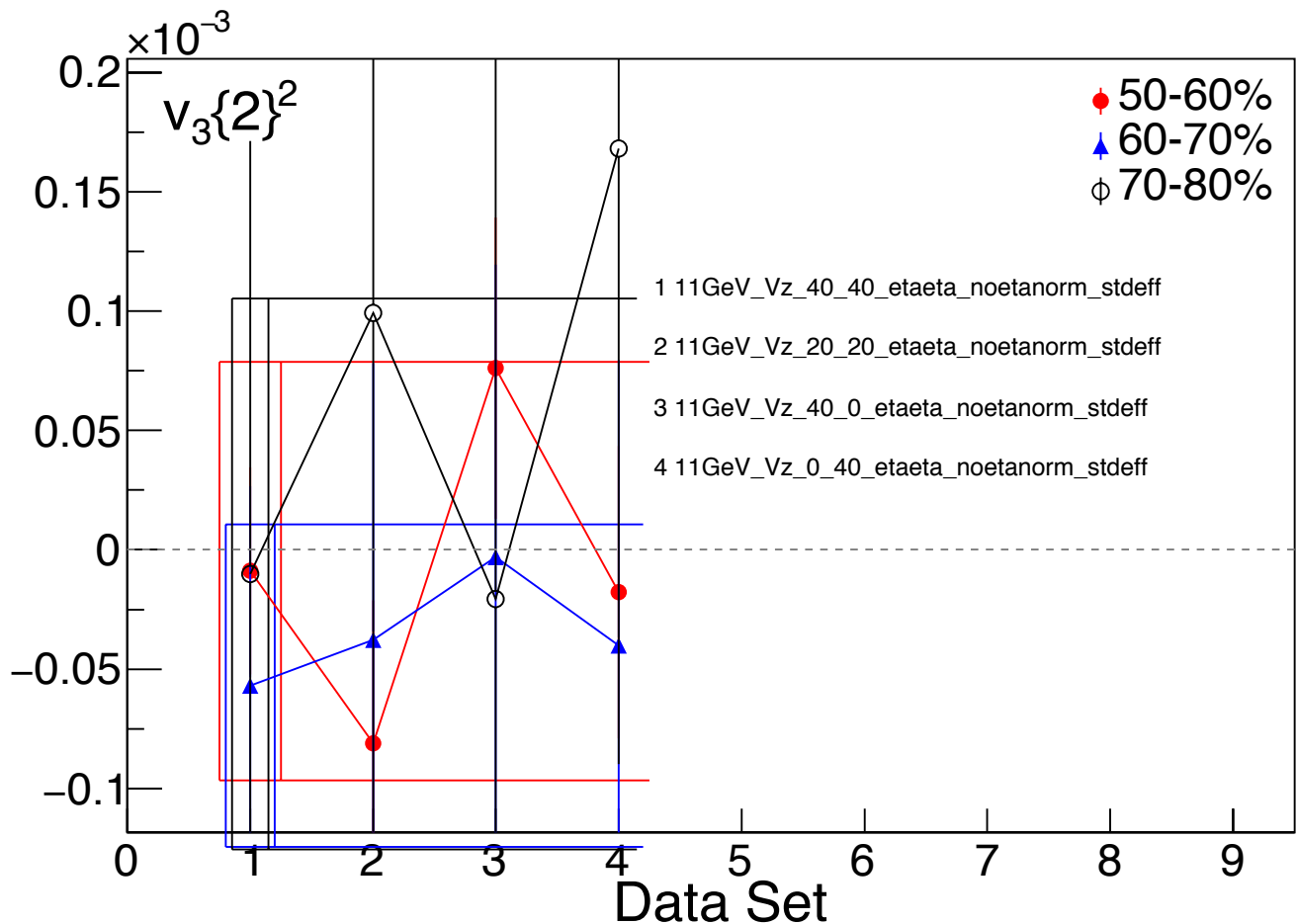
Systematic Uncertainty Estimates 14.5 GeV:



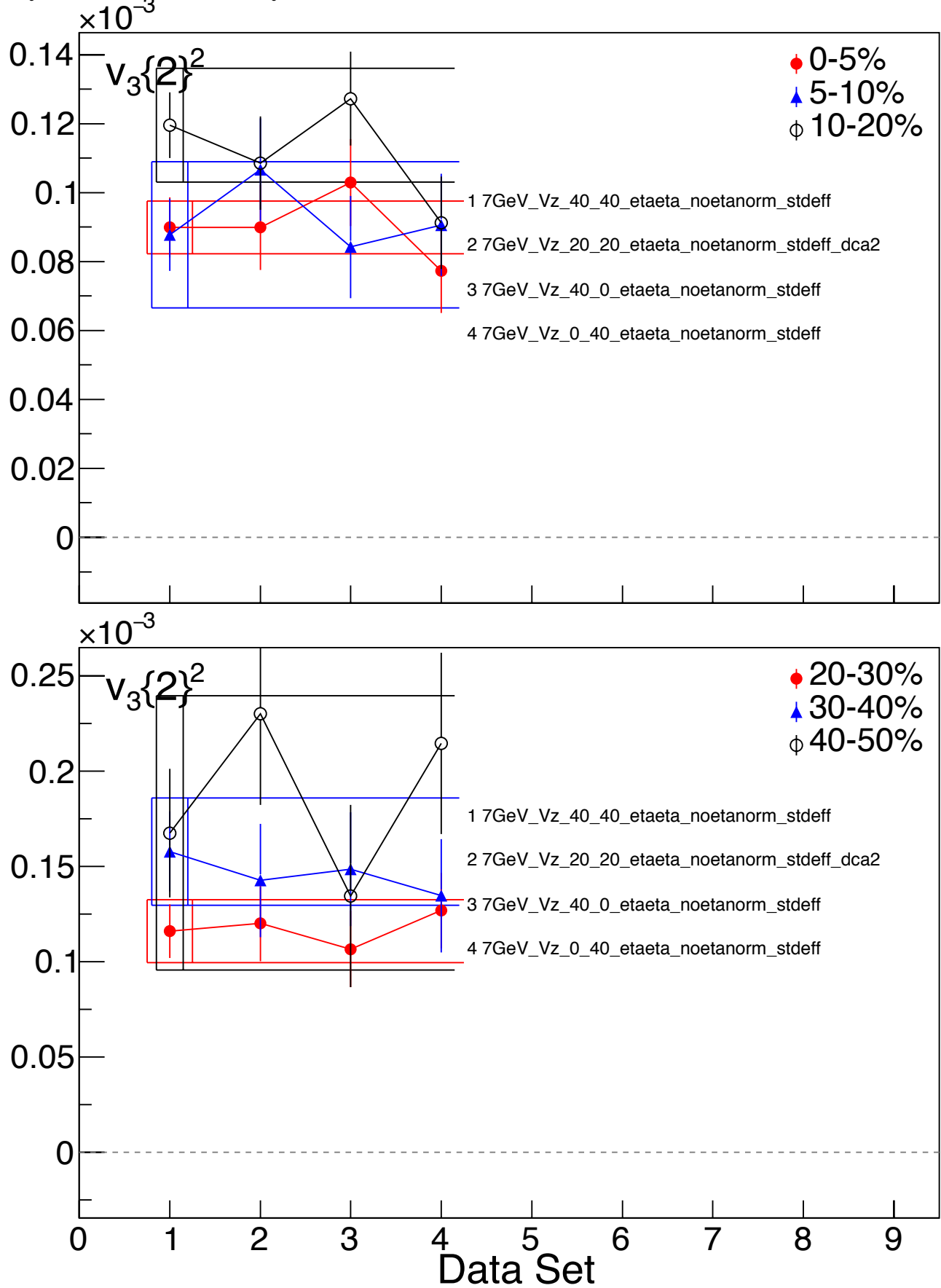
Systematic Uncertainty Estimates 11.5 GeV:



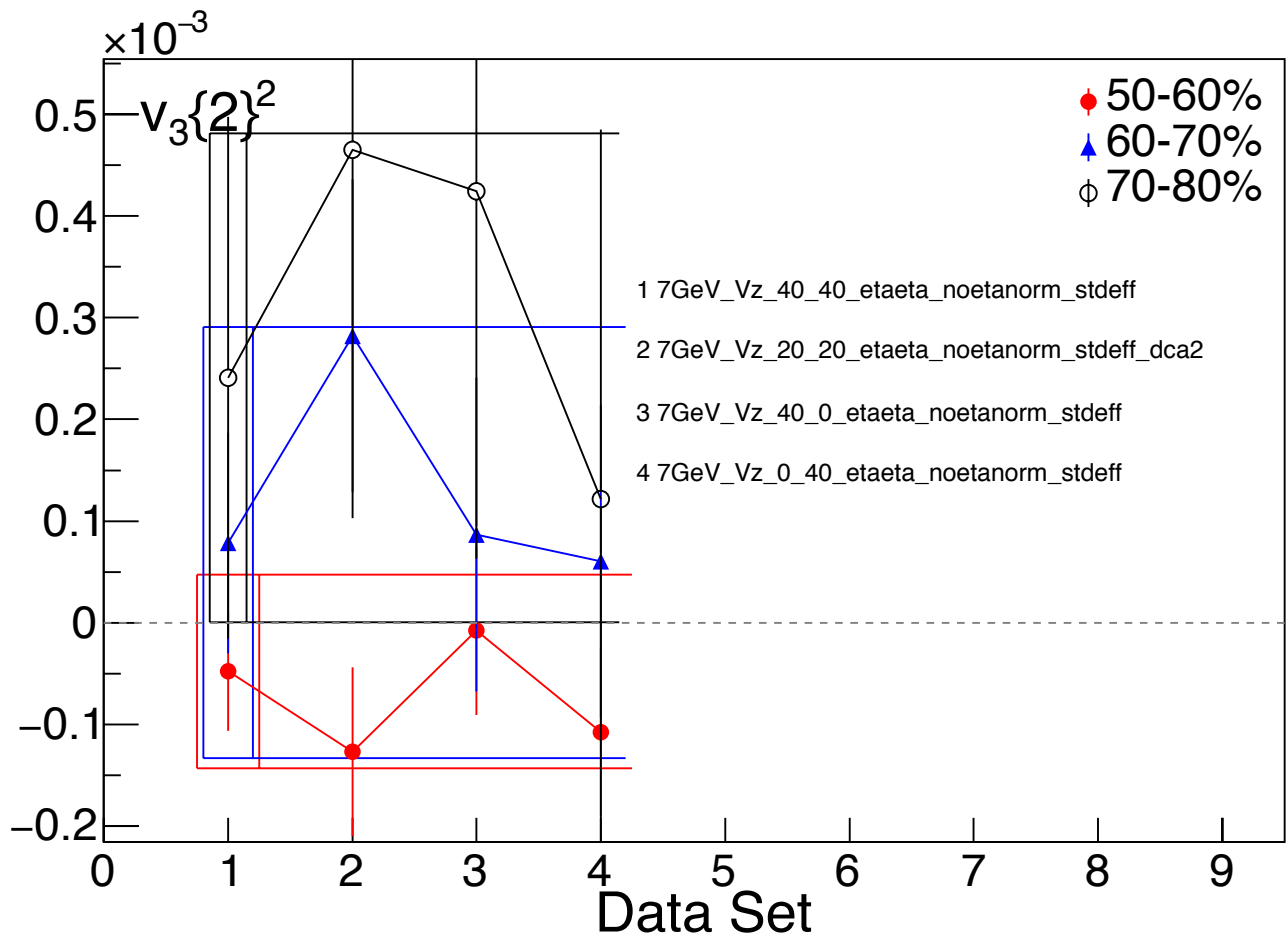
Systematic Uncertainty Estimates 11.5 GeV:



Systematic Uncertainty Estimates 7.7 GeV:

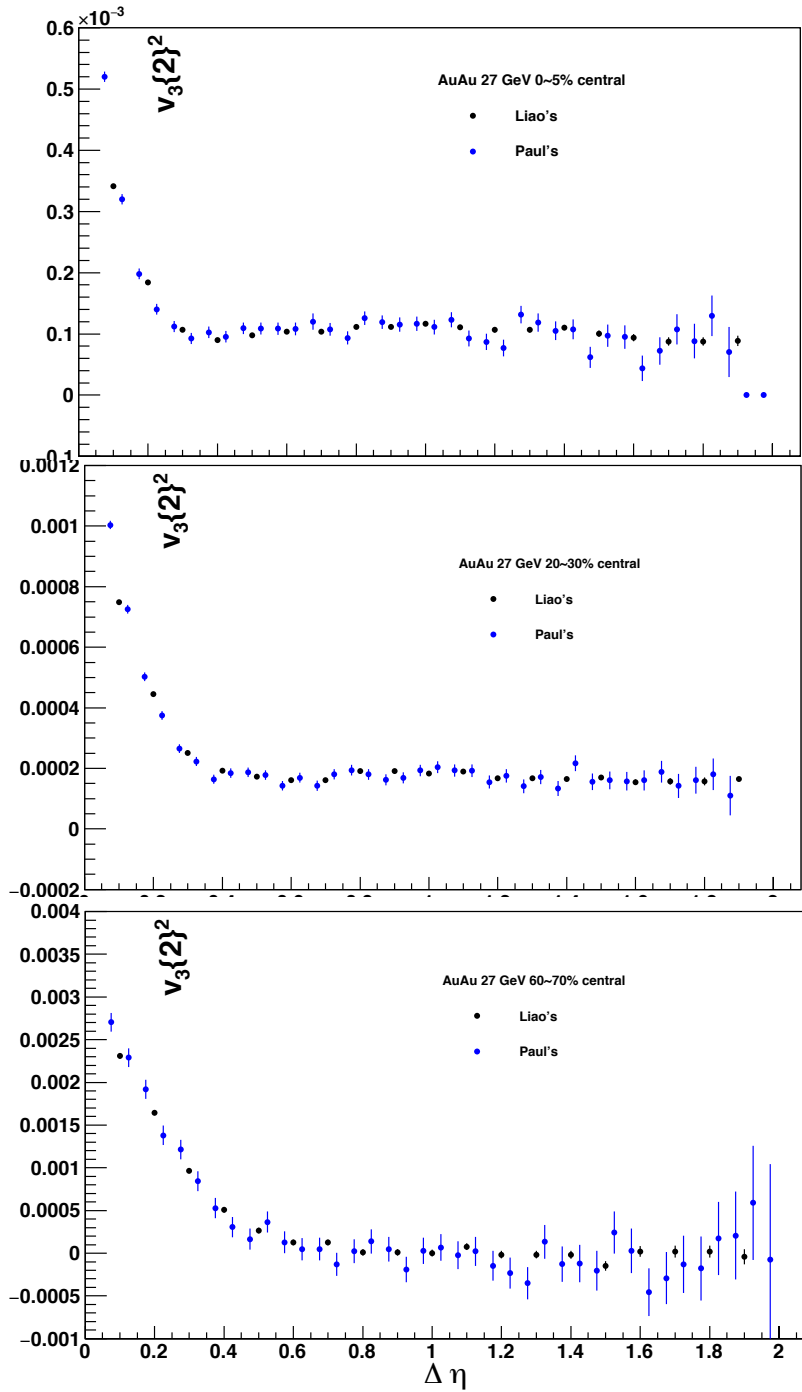


Systematic Uncertainty Estimates 7.7 GeV:



Systematic Uncertainty Estimates:

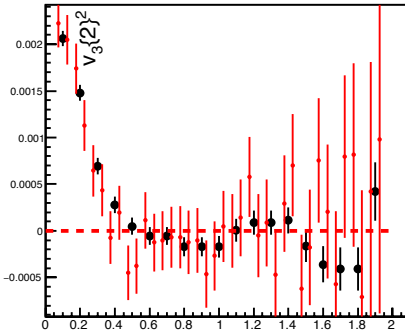
We've also investigated completely different analysis methods and found that they give almost exactly the same results. Here I show comparisons of the $\Delta\eta$ dependence of v_3 from Liao's event mixing technique where he reconstructs the two-particle correlation function then takes the 3rd harmonic. This is a comparison of three centralities for 27 GeV data. The two analyses agree very well.



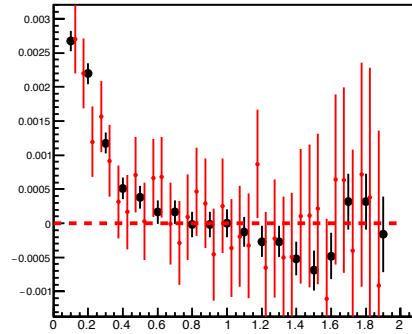
Systematic Uncertainty Estimates:

The paper also concludes that v_3 disappears in peripheral collisions at the lower energies, indicating that these low energy, low density collisions do not produce QGP. In order to verify this we've compared Liao Song's analysis (black) to Paul's analysis (red) for those bins. The comparison shows that our conclusions are robust. Niseem's data (lowest) also confirms the same behavior.

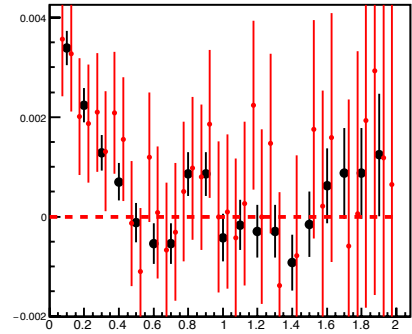
AuAu 7.7 GeV 50~60%



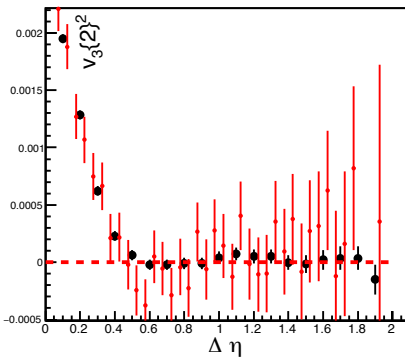
AuAu 7.7 GeV 60~70%



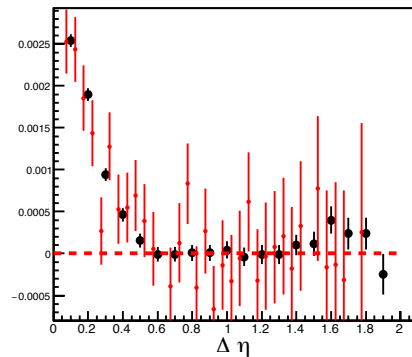
AuAu 7.7 GeV 70~80%



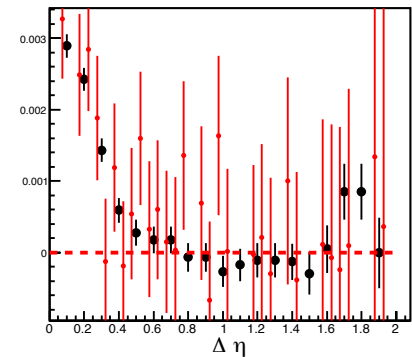
AuAu 11.5 GeV 50~60%



AuAu 11.5 GeV 60~70%

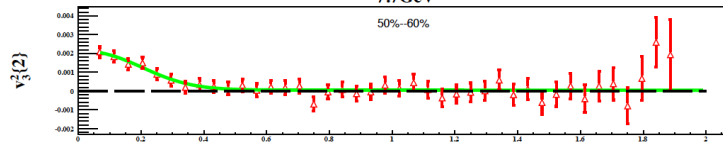


AuAu 11.5 GeV 70~80%



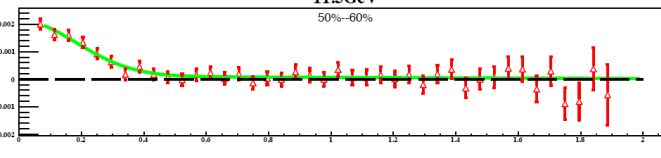
7.7GeV

50%~60%

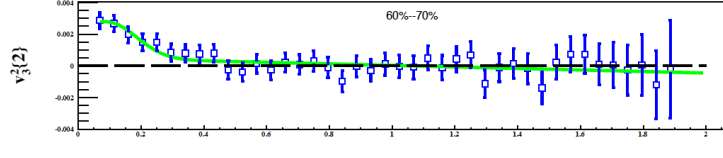


11.5GeV

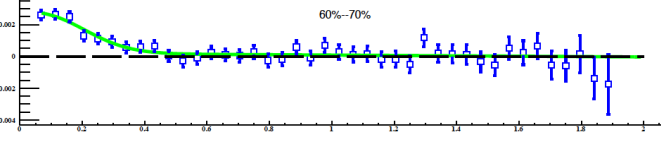
50%~60%



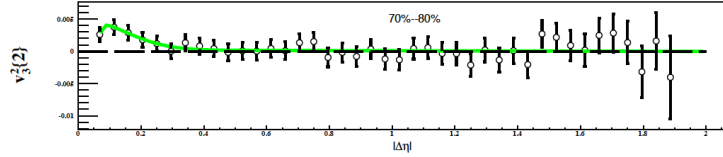
60%~70%



60%~70%



70%~80%



70%~80%

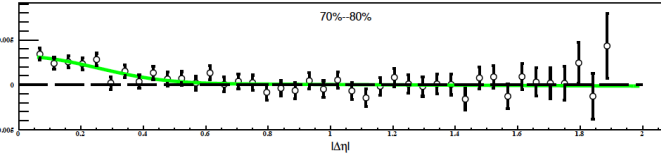


Figure 1:

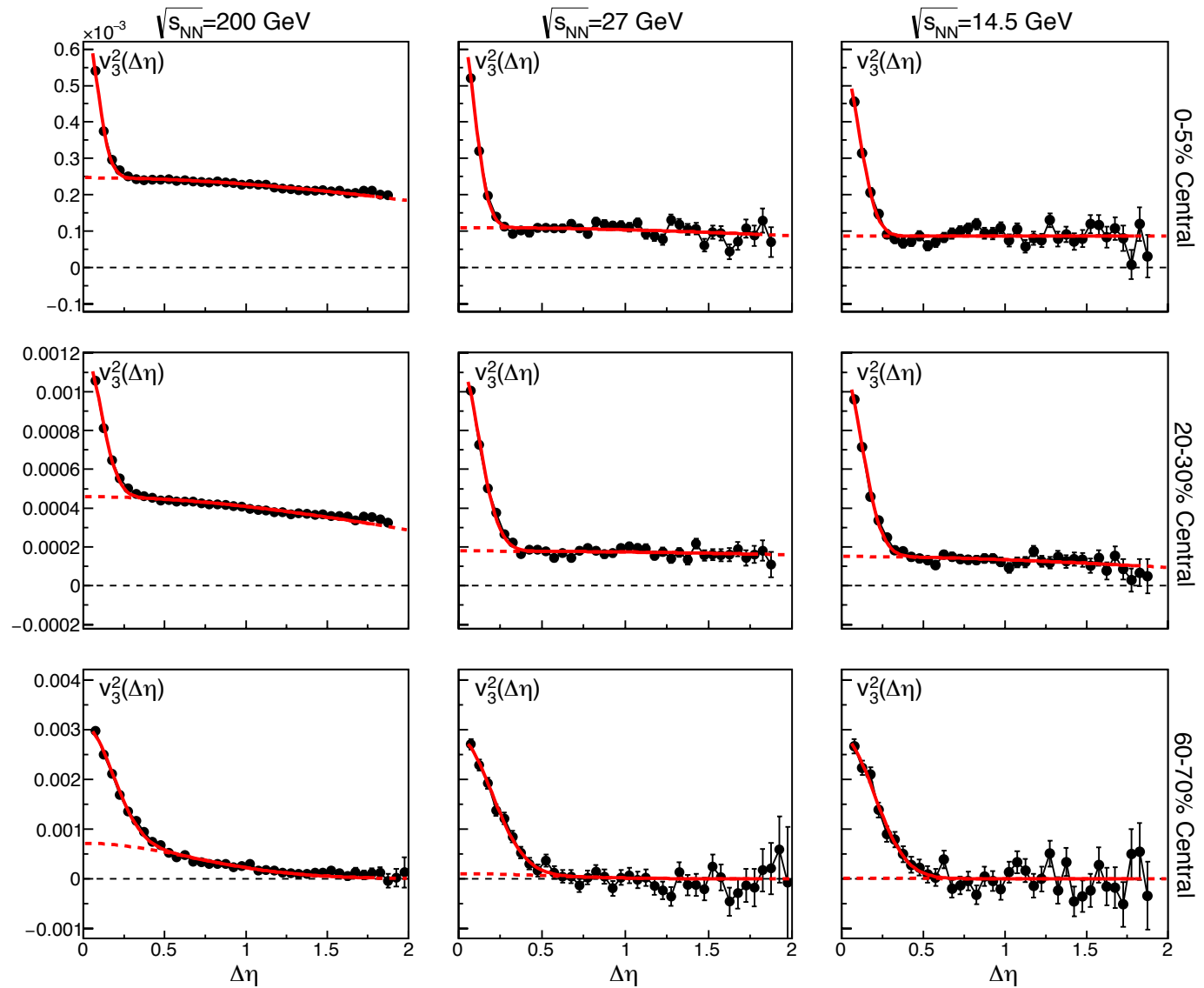


Figure 2:

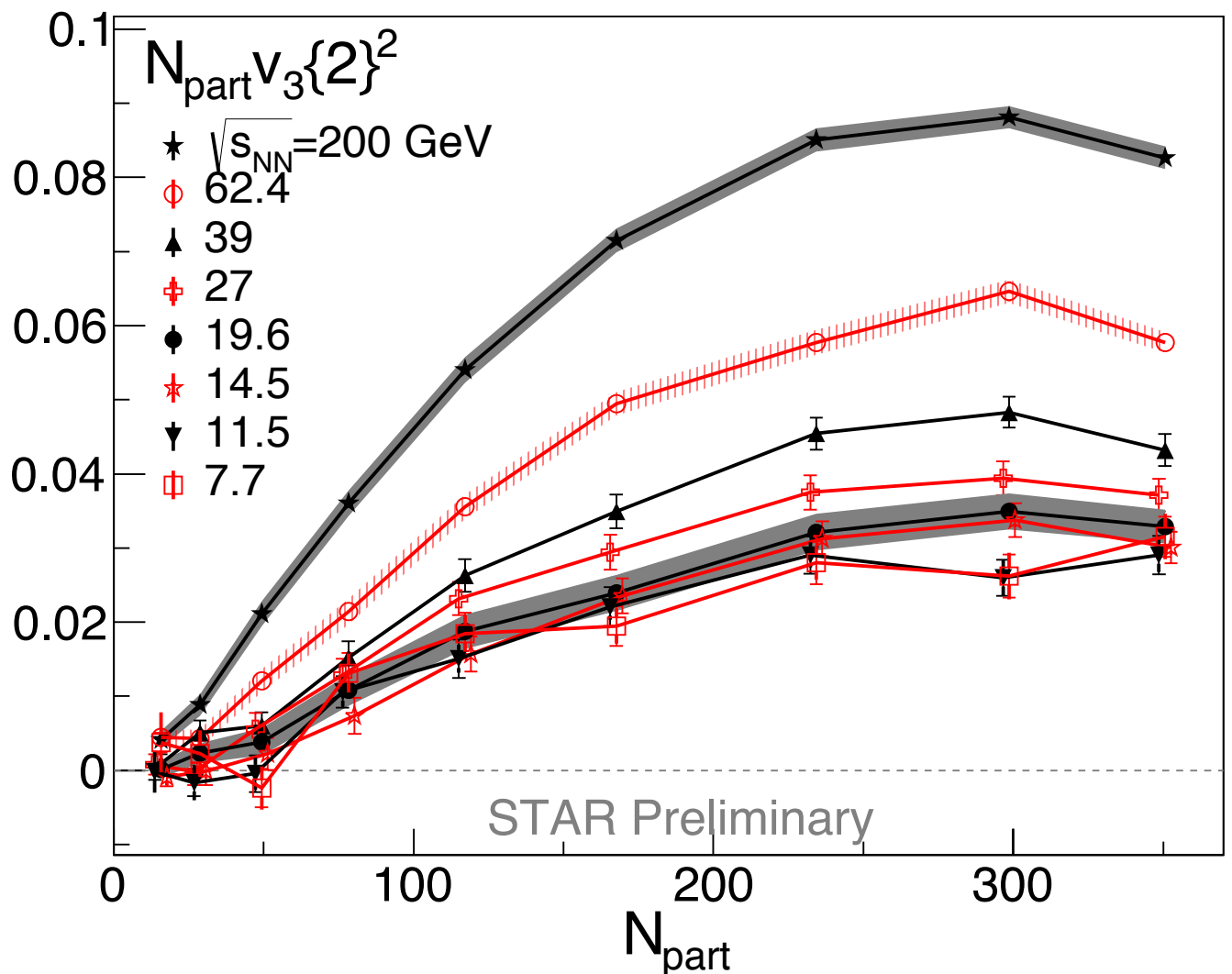
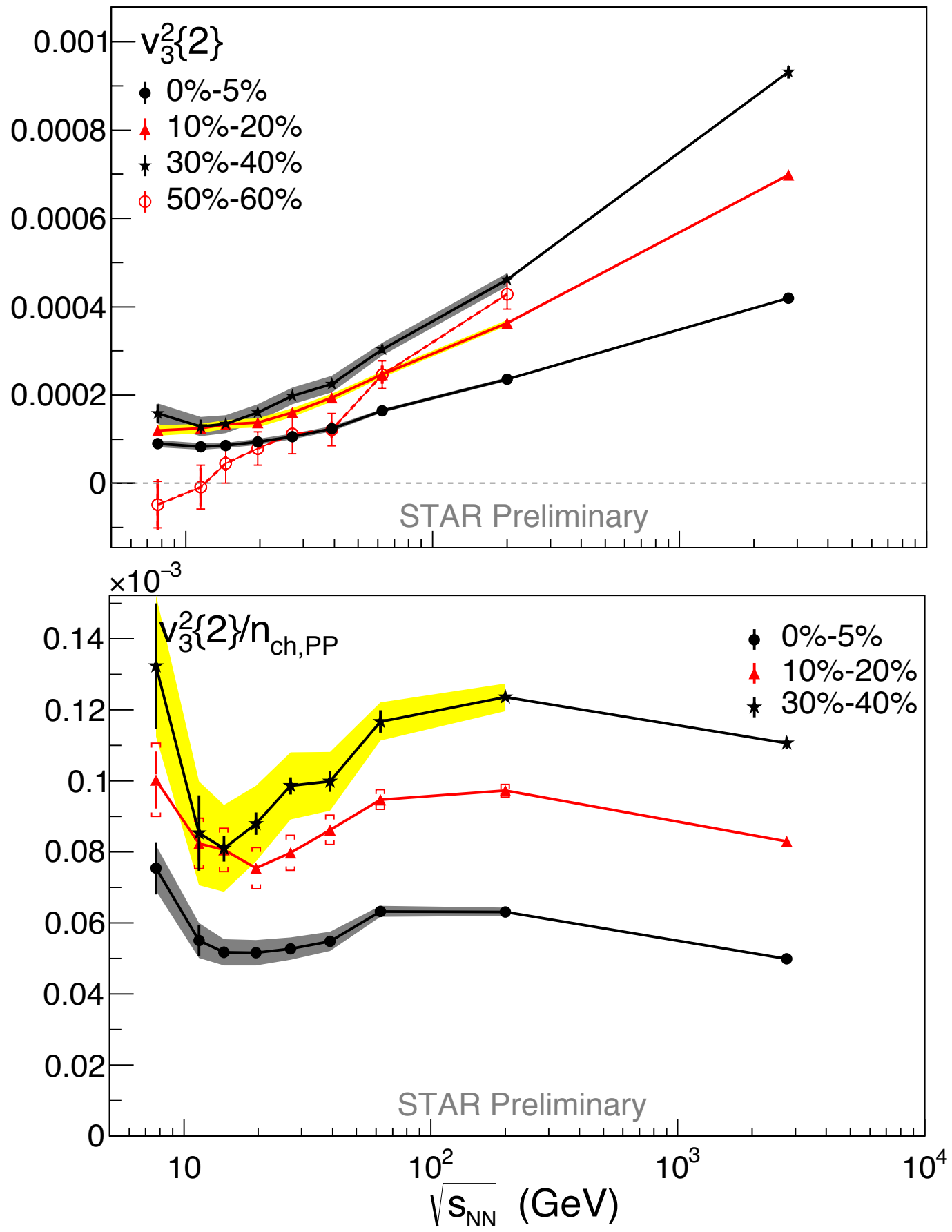
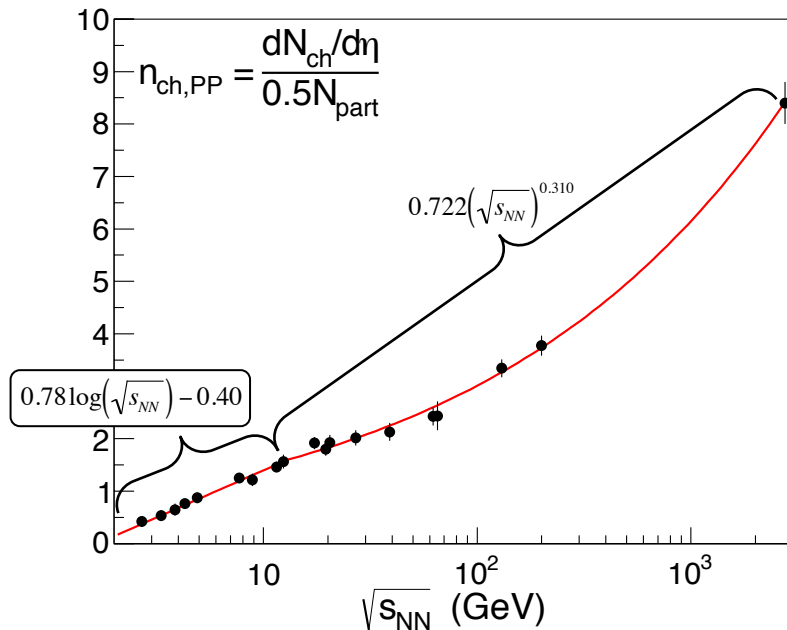


Figure 3 and 4:



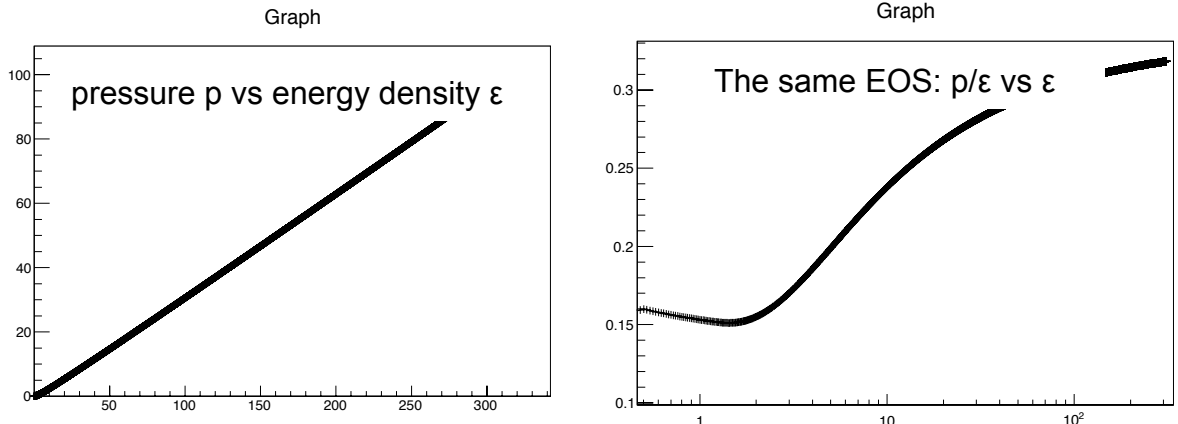
Auxiliary Studies:

Here is the parameterization used for $dN_{ch}/d\eta$ scaled by $N_{part}/2$. The parameterization does a very good job of reproducing the world's data including the preliminary STAR data in Evan Sangaline's thesis. The dip however is not strongly dependent on the exact parameterization. In fact the first time the dip was seen it was shown just using $\log(\sqrt{s})$ in the denominator.



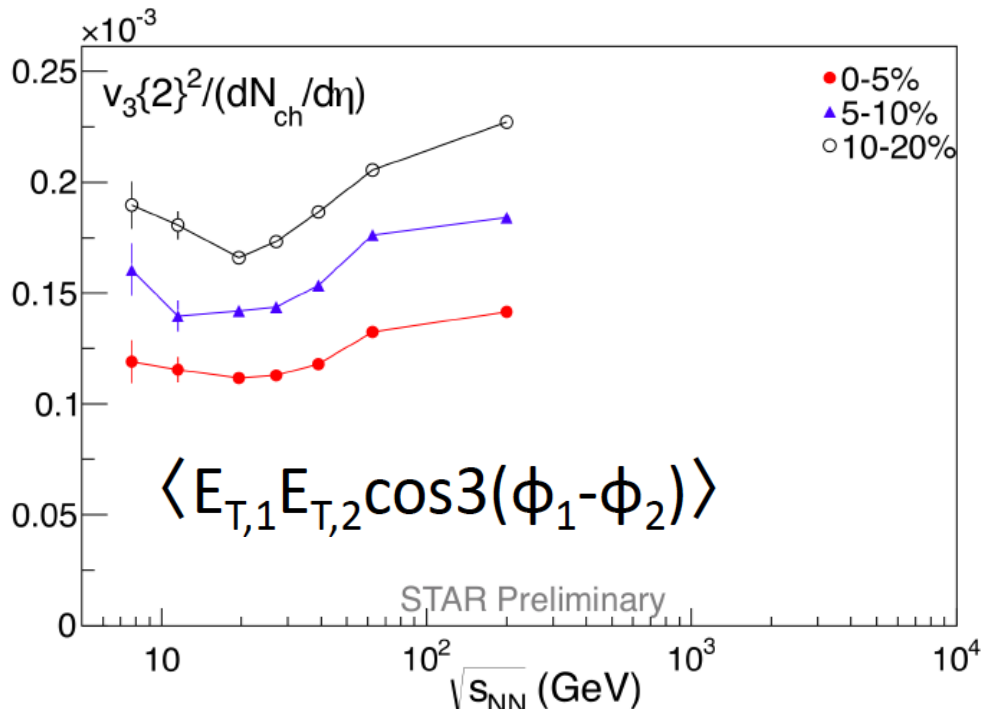
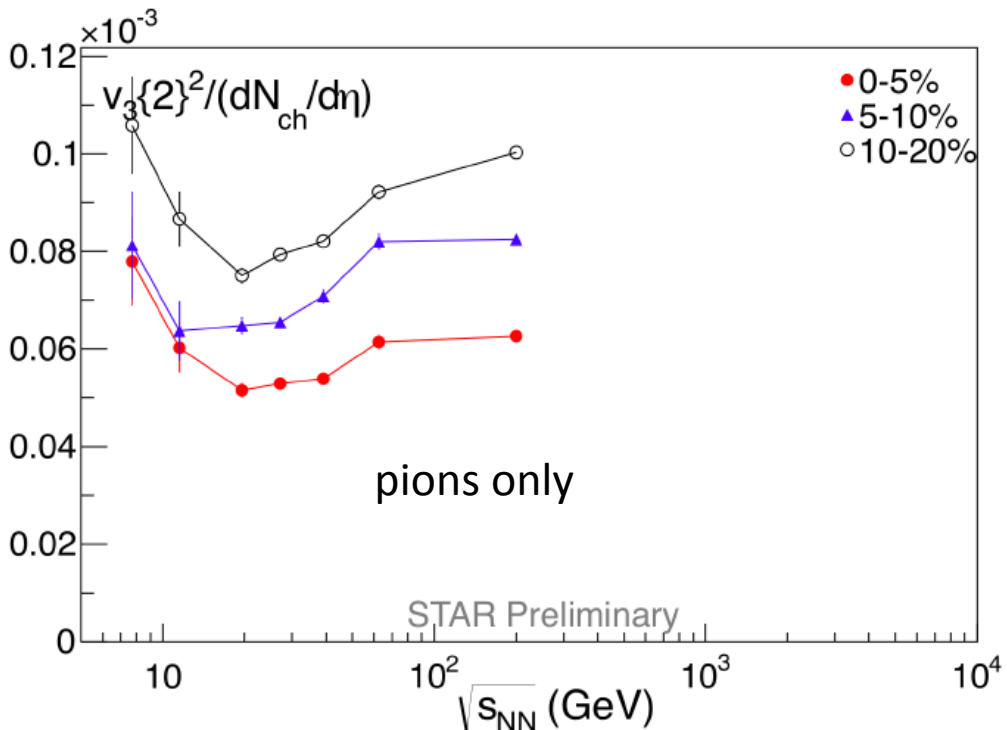
```
Double_t mult(Double_t x){ return (x>12.96) ? 0.7223*pow(x,0.310) : 0.78*log(x)-0.4;}
```

And what is the motivation for dividing by multiplicity? Sometimes a change in physics is only visible when we scale out trivial dependencies. Below as an illustration I show lattice QCD results for the equation of state. On the left is pressure vs energy density, on the right pressure/energy density vs energy density. Only the scaled results show any interesting trend.



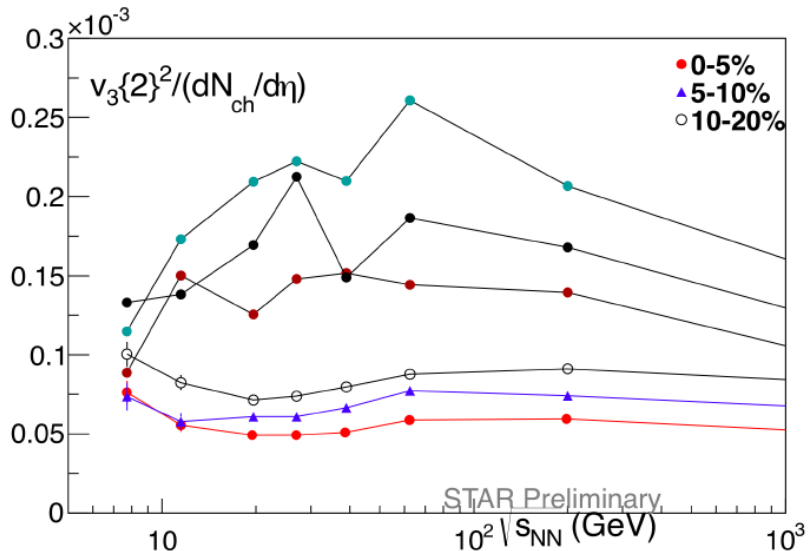
Auxiliary Studies:

Does the dip go away if you look only at pions? Can it just be related to changes in particle type and energy? The dip exists even when only pions are used and by looking at $\langle E_T^* E_T \rangle$ correlations instead of number of pair correlations, we see that the dip seems to be related directly to an asymmetry in “energy flow”.

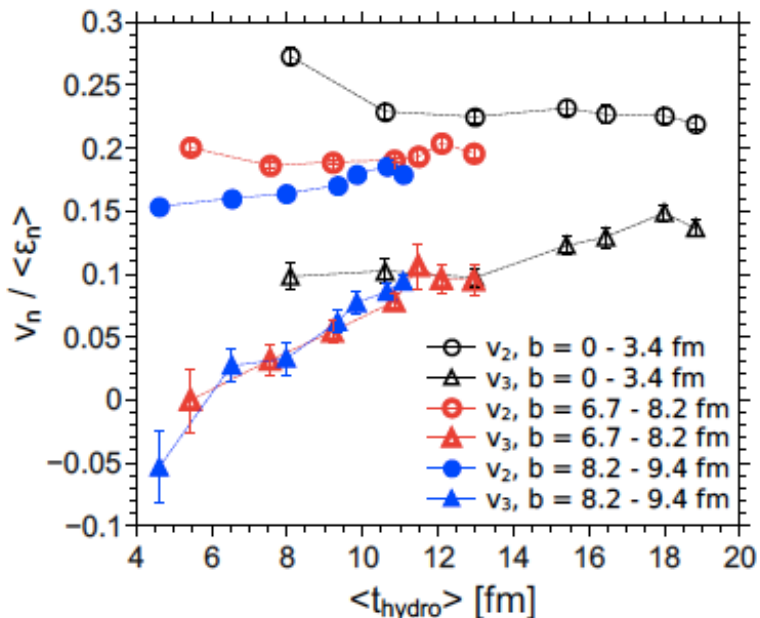


Auxiliary Studies:

Model comparisons. The AMPT model that is fairly good at describing vn data does not exhibit this dip.

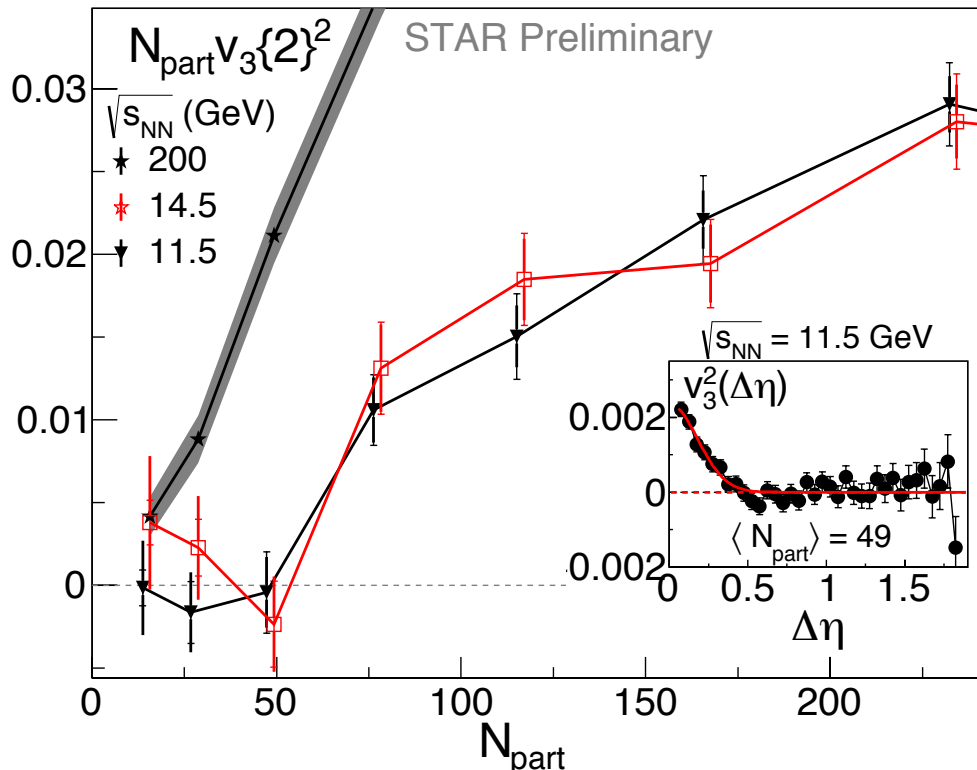
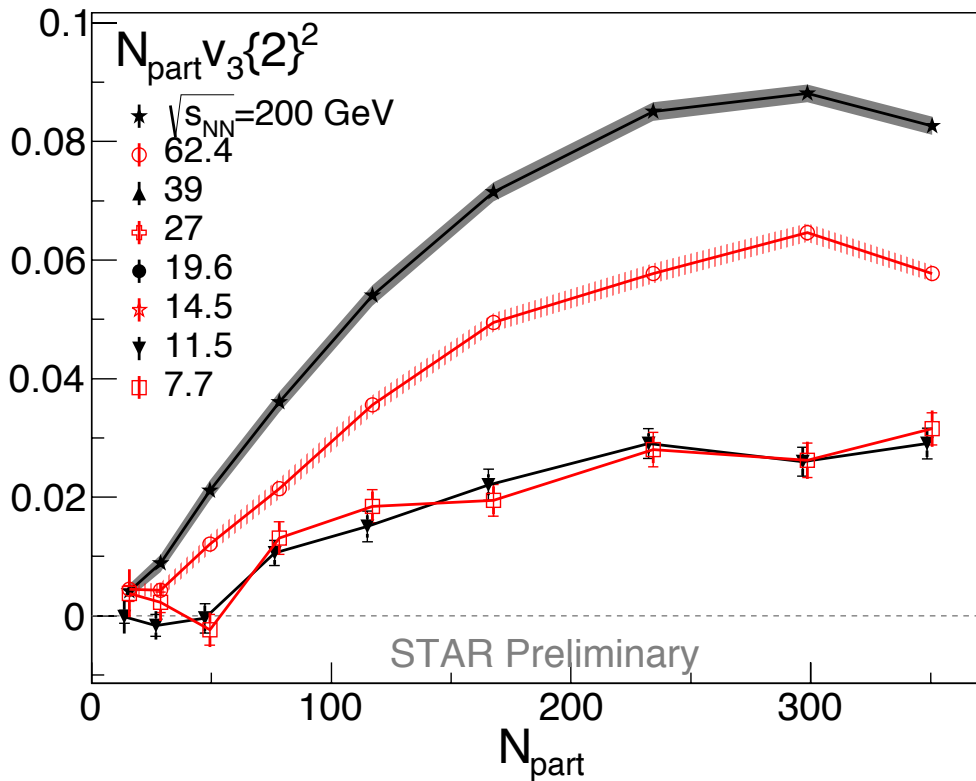


Here is the figure that shows a hybrid model calculation of v2 and v3. Results for different centralities and energies are plotted vs the duration of the low viscosity hydro phase. While v2 is barely correlated with the duration of the hydro phase, v3 depends strongly on the existence of a low viscosity hydro phase and grows as the duration of that phase grows. This supports the argument in the paper that v3 is more sensitive to the existence of a low viscosity plasma phase.



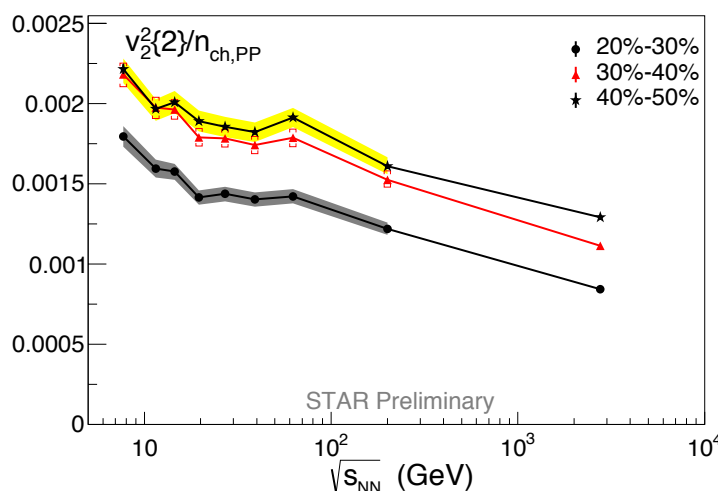
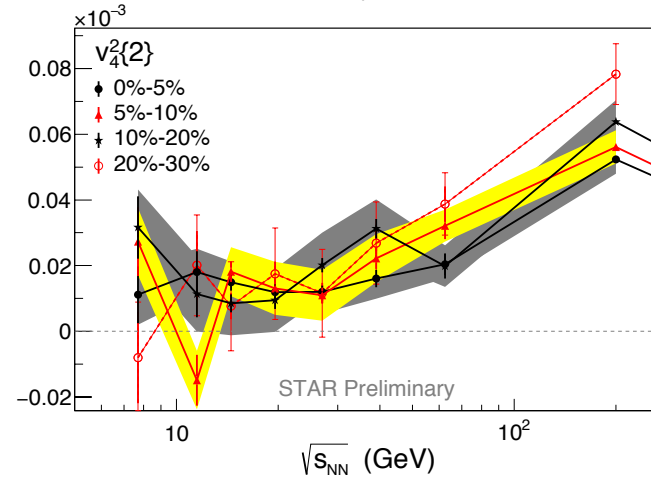
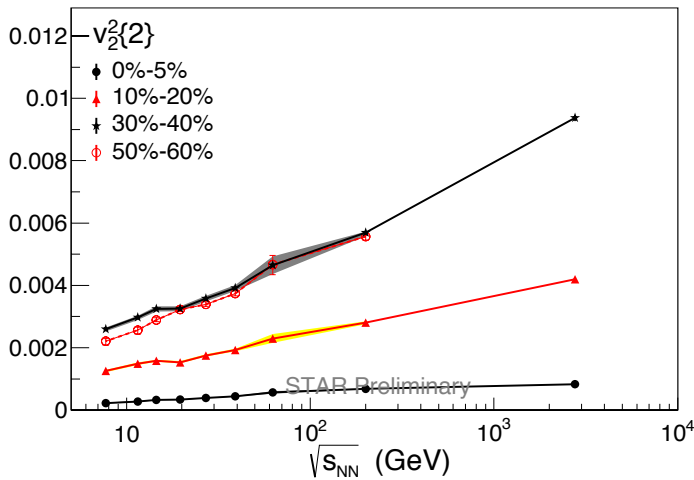
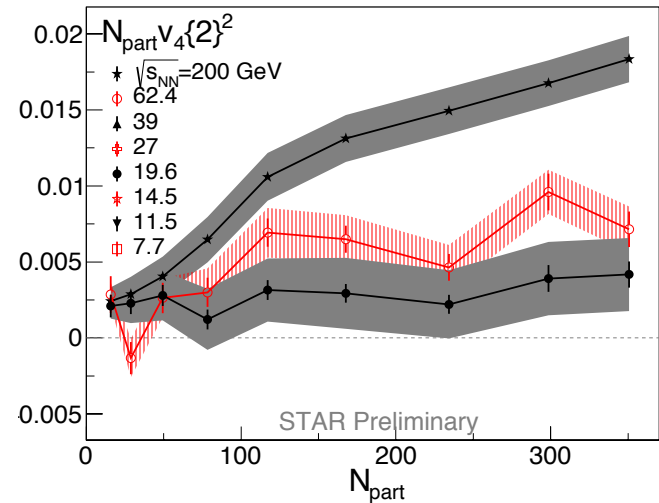
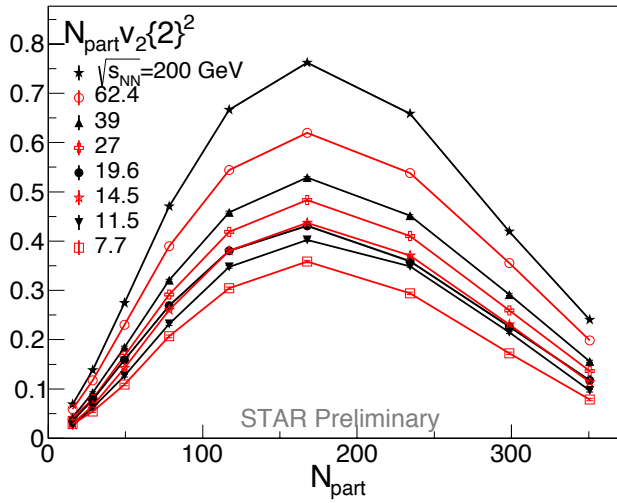
Auxiliary Studies:

Here are some figures to help show that v_3 goes away in peripheral collisions at lower energy. The fits vs $\Delta\eta$ also show the disappearance of v_3 .



Auxiliary Studies:

Below we show results on the centrality and energy dependence of v₂ and v₄. At the bottom left we also show $v_2^2\{2\}$ scaled by $n_{ch,PP}$.



Note on Sagita:

We use the equation from Blum and Rolandi to convert 0.5 Tesla into radius of curvature r for a given pT. Then given r and the size of the TPC, we derive the sagita. We choose this variable since it has a fairly direct impact on the region of the TPC a given track will traverse.

$$s = r - \sqrt{r^2 - l^2}$$

For a 0.5 Tesla Field

$$s \approx \frac{20 p_T}{3} - \sqrt{\left(\frac{20 p_T}{3}\right)^2 - l^2}$$

Blum and Rolandi: "Good to better than one tenth of a percent"

